Enhancing the efficiency of High-Temperature storage by reducing the effect of density-driven flow

A case study of High-Temperature storage on the TU-Delft campus

By

Vincent Leclercq
4283732

in partial fulfilment of the requirements for the degree of

Bachelors of Science
in Civil Engineering

Supervisors: Ir. Martin Bloemendal
Ir. Bas des Tombe

TU Delft

Acknowledgments

I would like to thank my supervisor Ir. Martin Bloemendal and Ir. Bas des Tombe for helping me throughout the production of this thesis. They always provided great and efficient advice on how to tackle my research. I would also like to thank Sanne de Smet for providing a constructive peer review halfway through the project. Finally I would like to thank the reviewer of this paper for taking the time to evaluate the quality of my work.

Abstract

This thesis goals to assess the effect of density driven flow in an Aquifer Thermal Energy Storage on the TU Delft, by using groundwater from a deep aquifer for a hot storage in a more shallow layer. During storage the hot water source will have a density closer to the density of ambient groundwater. This reduces the effect of free density.

Density of water in the subsurface was found to be dependent on salt concentration and temperature of water. A geothermal gradient of 20℃/km and a storage temperature of 60℃ were followed. Due to lack of data a salt gradient range of 17 mg/L to 77mg/L, with a reference value of 35 mg/L.

Possible layers for HT-ATES in Delft were determined by Hacking (2017) under reserve of further research concerning the properties of the soil in the aquifers. The three layers that are compared are the Maassluis formation (160m depth), the Berg Sand formation (420m depth) and the Texel Greensand Member (560 m) The tilting time was found to be greatly dependent on the hydraulic conductivity of the soil. The effect of the solution will therefore be dependent on further research on these parameters.

A density-difference compensation of 60% was estimated in the reference case of the study, by using water from the Texel member as storage in the Maassluis formation. Increase in tilting time of 170% was estimated for this reference case. The tilting time improvement was found to be drastically maximized when the cold storage was closest to the optimum density difference compensation depth. More research should therefore be carried out on the actual salt gradient present in Delft. In combination with an accurate soil hydraulic conductivity this data can be modelled to assess the recovery temperature of the HT-ATES

Symbol list

Symbol	Symbol name	Unit
A	Pre-exponential factor	[s-1]
Ca	Heat capacity of aquifer soil	[J/(K m3)]
Cs	Salt concentration	[kg/m3]
Cw	Heat capacity of water	[J/(K m3)]
D	Aquifer depth	[m]
DDC	Density difference compensation	[%]
Ea	Activation energy	[kJ/mol]
ε	System efficiency	[-]
g	gravitational constant	[m/s2]
G	Catalans constant	[-]
H	Aquifer thickness	[m]
k	Reaction rate	[-]
kah	Horizontal hydraulic conductivity	[m/s] [mD]
kav	Vertical hydraulic conductivity	[m/s] [mD]
M	Mixed convection ratio	[-]
ρ	Density	[kg/m3]
ρ0/ρa	Ambient water density	[kg/m3]
ρ1/ρs	Storage water densityt water density	[kg/m3]
$\Delta\rho_i$	Initial density difference in layer	[kg/m3]
Δρf	Density difference after compensation	[kg/m3]
R	Universal gas constant	[J/(mol K)]
r0,05, bottom	initial radius to the 5% isochlor	[m]
R*	Recoverability ratio	[-]
Ra*	Adapted Rayleigh's number	[-]
θ	Porosity	[-]
S	Salinity	[-]
T	Water temperature	[˚C]
Ta	Ambient water temperature	[˚C]
Ts	Storage water temperature	[˚C]
Tp	Extraction water temperature	[˚C]
Ti	Injected water temperature	[˚C]
μ	Dynamic viscosity of water	[kg/(m s)]
μ0	Dynamic viscosity of ambient water	[kg/(m d)]
μ1	Dynamic viscosity of storage water	[kg/(m d)]
Vp	Extraction water volume	[m3]
Vi	Injection water volume	[m3]
vfree	Theoretical velocity of flow induced by free convection	[m/s]
vforced	Theoretical velocity of flow induced by forced convection	[m/s]

Figure list

Table list

Content table

1. Introduction

1.1. Problem description

In a world where the demand for sustainable sources of energy is growing, the Netherlands have presented the objective to transition to 16% of sustainable energy by 2023. By 2050 the production of C02 related to the energy production of the Netherlands should be shrunk to 80-95% compared to the emissions of 1990 (Rijksoverheid 2017)[i] . When looking at the distribution of energy demand in the Netherlands we see that energy required for heat and cooling of industrial buildings and households still accounts for 25-40% of the total energy consumption of the Netherlands (Jong, 2016)[ii] . A huge step toward achieving the 2050 goal can therefore be made by eliminating this emission source.

The magnitude of the actual problem has led to the development of new heat recovering technologies in the sector of solar-,bio-, and geothermal energy in order to help achieve this transition. Also with the apparition of smart grids heat recovered from industrial waste can now be used with more ease, offering new sources of energy that were inaccessible before.

In order to be able to use these new heat sources efficiently a need for heat storage rises, coupling the heat offer to the demand. Geothermal storage can be an excellent way to provide a buffer for a peak in heat offer or demand, bridging over seasonal variations of heat production/ demand. Figure [1] shows that thanks to geothermal storage of excess energy, the average heat demand of a building can be diminished by as much as 16%.

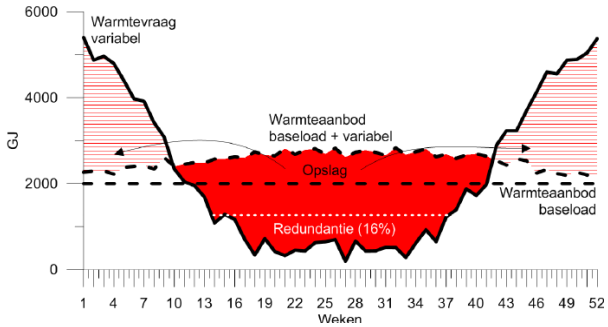

Figure 1 Example of buffer function of a geothermal storage by Hartog et al., (2016)[iii]

The TU Delft has been a pave craver for projects focussed around energy transition, and through this optic "Het Delft plan" was started, aiming to show that the Netherlands can be on the forefront of European energy offer, storage and transport[iv] . A part of this project focusses on the storage of heat from geothermal energy in aquifers under the campus of the TU Delft, in cooperation with the DAP (Delft Aardwarmte Project, 2017[v]).

Two types of temperature storage can be distinguished: Low temperature Aquifer Thermal Energy Storage (LT-ATES)and High-Temperature Aquifer Thermal Energy Storage (HT-ATES). LT-ATES are already widely used throughout the Netherlands and have proven to provide a viable. More than 2000 installations are already in place as was shown by Willemsen, (2016)[vi] . The storage temperature refers to the temperature of the water injected in the aquifer. Most LT-ATES have a storage temperature under 25 ℃, due to governmental regulations concerning storage in drinking water. This low temperature cannot be used directly to provide heat for building. It is required to use a heat pump in the system, consuming up to 60% of the total energy required for the system as was researched by Dekker, (2016)[vii] . Storing water at high temperature (>60 ℃) enables the system to heat a building directly. Great system efficiency improvements can therefore be gained by storing water at high temperature (>60 ℃).

Storage of high temperature water in an aquifer does create problems that need to be investigated. One of these is related to the density difference between hot and cold water in the same aquifer: free convection. Hot storage water is lighter than ambient cold water. Buoyancy forces cause the hot water to flow up, thereby tilting the front between hot and warm water. On the one hand this leads to extra conduction of heat on the border between the hot and cold water, since the contact surface between the two increased due to the tilting. On the other hand, the viscosity of the hot water is lowered due to the high temperature, resulting in a free convection that is easier than with lower temperature water. This leads to a localised convection flow of water, mixing the hot and cold water, thereby reducing the efficiency of the overall system.

1.2. Goal

The goal of this thesis is to reduce the effect of free convection in a High Temperature-Aquifer Thermal Energy Storage (HT-ATES) by reducing the difference in density between the hot and cold water storage. Groundwater tends to enhance in density with depth due to increase in salt concentration. Water with a higher density from a deeper aquifer will therefore be used as hot water source to compensate density difference.

1.3. Approach

In order to enhance de efficiency of the future HT-ATES on the campus by reducing the effect of free convection, different storage systems will be presented. This will show different factors influencing the efficiency of a HT-ATES. A system that aims to counteract the effect of free convection will then be presented. It uses water of higher density than that of the cold ambient water at same temperature, which will, during storage at high temperature, reduce the density difference. This will lead to less free-convection losses.

In Chapter 3 the density of groundwater as a function of salt content and temperature will be researched.

Hacking, T. (2017)[viii] studied the feasibility of a HT-ATES on the campus, and concluded that 4 soil layers could be suitable to store high temperature water. His analysis will serve as a basis to evaluate which combination of layers would be most suitable to reduce the effect of free convection in Chapter 4.

In Chapter 5 the augmentation in efficiency of the system based on an initial situation in the aquifer chosen in Chapter 4 will be evaluated. Assumptions of vertical conductivity will be made in order to predict the final efficiency.

Finally a discussion will be carried out to enlighten possible sources of errors in the study. A conclusion will also be drawn on the economic feasibility of this concept.

2. Aquifer Thermal Energy Storage description

In this chapter different types of ATES will be presented. This will highlight the main difference in system between aquifer temperature storages, and advantages and drawbacks of each. After that the promising points of high temperature ATES will be highlighted. A short overview of factors affecting the efficiency of such a system will be delivered. Finally we will illustrate the system on which we are going to we are going to base our case study: an open HT-ATES monowell with a deeper laying aquifer for cold storage than hot for the hot storage.

2.1. ATES Presentation

An Aquifer Temperature Energy Storage system goals to store heat in an aquifer, in order to recover it when it will be needed for the heating of buildings. On the same principle, cold water can also be injected in order to provide cooling. These systems are efficient for climate control in buildings like offices, housing or greenhouses. In most cases the buildings are heated using gas installations, therefore ATES provide a sustainable option for climate control in a building.

Different systems of ATES systems exist, the most common ones being doublet systems and monowells. However some design incorporate an extra well of medium temperature storage (triplets) in order to conserve the high energy value of water at 60 ℃ . This enables a heating approach that is better designed to the season in which the building needs to be heated. In the next paragraphs we will discuss the different types of well combination for ATES.

2.1.1. ATES Doublets

The most basic system of wells to store heat in an aquifer is a doublet. As the name states, the system consists of two wells placed at approximatively 100m of each other, in the same aquifer. An ATES consists of a hot and a cold storage. One well is therefore used to store hot water, while the other stores cold water. During the winter hot water is extracted from the aquifer. In the summer the process is reversed, and the cold source is used as cooling for building (Sommer,2015[ix]) . The hot water is often stored in the same aquifer as the cold storage, but this is not always the case. This system is schematised in Figure [2].

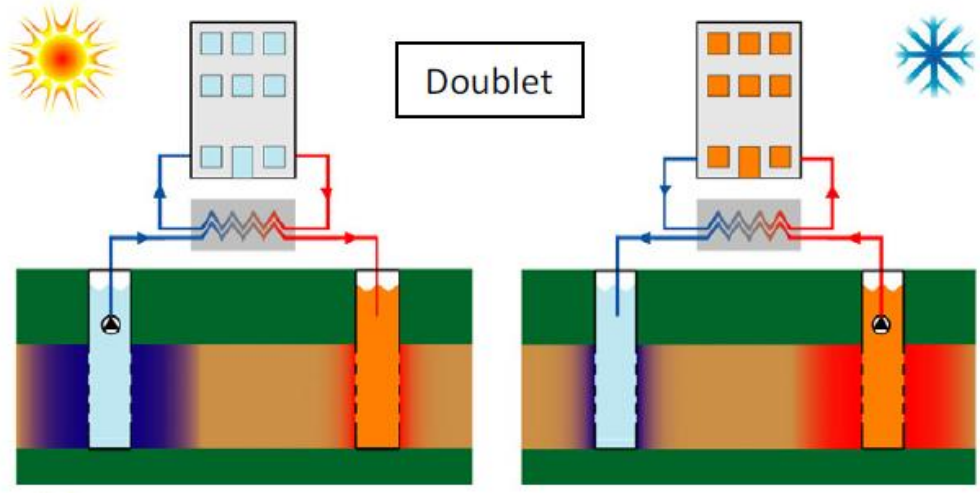

Figure 2 General functioning of ATES Doublet by Calje, (2010)[x]

2.1.2. ATES Monowells

Another well system for temperature storage in an aquifer is a mono-well system. In this case the same well is used to extract hot and cold water from aquifer(s). The injection and extraction pipes for hot and cold storage are separate in the well casing to permit the system to function. A structural schematisation of a monowell is presented in Appendix [1]. In this system hot and cold storage are often separated by an impermeable layer, typically an aquitard. The obvious advantage of this system is that there is only one well

required for the storage. This decreases the purchase costs of the system. If the storage aquifer is thick enough, an aquitard is not even needed. The hot water can be stored in the top layer of the aquifer, while the cold water is stored at the bottom. Special note should be taken not to inverse these two, since hot water will tend to flow upwards due to buoyancy.

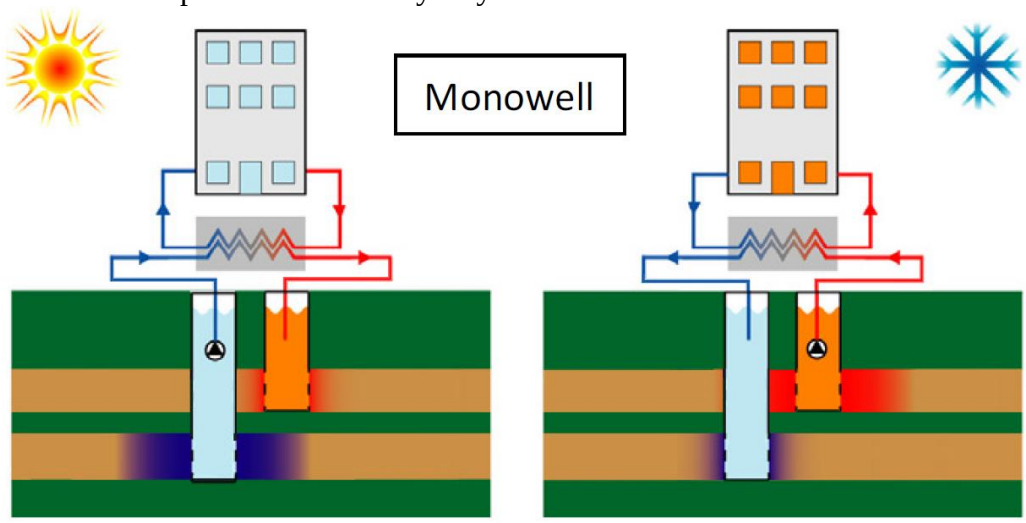

Figure 3 Monowell system schematisation by Calje, (2010)

2.1.3. ATES Triplet

The last system we will observe is a triplet system, as it was described by Bloemendal, et al., (2016)[xi]. A triplet is composed of three wells. As in a doublet or monowell system, a hot and cold storage are present. This system differentiates itself from the systems mentioned above by the presence of a third well of medium temperature. The idea behind this system is that to heat or cool a building effectively, we need water temperatures that are designed to the season. In some situations there will be an excess of shortage of heat, depending on the outside temperature. Since these excesses are usually moderate in temperature, and are preferably stored in order not to get lost, it becomes wishful to add another well of medium temperature. This prevents pollution of the cold or hot well. A visual representation of a triplet system is presented in Figure [4].

Typically a triplet system's strength lies in autumn and spring. Supposing that the outside temperature is too low to leave the building unheated, but the reflux source is too hot to be used directly as cooling in the summer. The reflux source can be stored with a third well, where it will not enhance the temperature of the cold storage. Similarly, when the outside temperature is too high to leave the building uncooled, the reflux source will have a temperature that is too low to be injected in the hot water well. The third medium temperature storage will now prevent pollution of the hot storage.

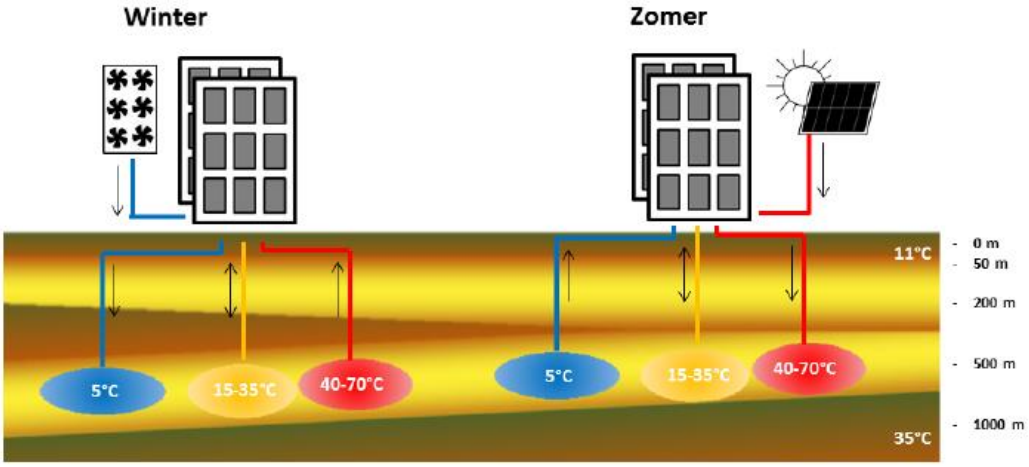

Figure 4 Functioning principal of a HT-ATES triplet by Hartog et al (2016)

A triplet system is more effective in a HT-ATES than in a LT-ATES. In the case of a LT-ATES a heat pump is needed to enhance the temperature of the hot storage to a temperature that is usable for the heating of a building. This means that the purity of the hot source is already compromised in the case of a LT-ATES, reducing the importance of a third well. It is nonetheless important that the cold well remains of low temperature. In case of a HT-ATES a heat pump becomes obsolete. This enhances the importance that the stored water remains at a high temperature, since the building will not be able to be heated properly if the storage temperature becomes too low.

2.1.4. Low or High Temperature Storage

Heat and cold storage being a bridge between seasonal heat demand fluctuations, it is not surprising that as much as 2000 ATES have already been implemented in the Netherlands (Energievastgoed, 2017[xii]). Almost all of these systems are now for low (around 20 ℃)or medium (<60 ℃) water temperatures. The cold storage is preferably at temperature between 5 ℃ and 10 ℃. The terms of low and medium temperature are expressed in comparison to the ambient temperature of the water in the soil (≈10 to 13 ℃)(Bloemendal, 2016) .

The reason why so many LT-ATES are in implementation is due to their recovery efficiency and their low price. The heat recovery of a LT-ATES is high (75-90%) compared to a HT-ATES (50-90%) (Hartog et al, 2016). Its low price follows from the relatively shallow depth at which the system is implemented, between 25 and 250m, reducing the costs of the well placement(Calje, 2010) .

A major drawback of LT-ATES follows from the recovery temperature. As stated before, LT-ATES have a storage temperature around 20 ℃. This is too low to heat a building directly. A heat pump is therefore needed to enhance the temperature. This creates a drawback from an environmental point of view, as this heat pump consumes as much as 60% of the total energy cost of the system (Dekker, 2016). Because of this high energy demand a LT-ATES becomes less efficient as a way of storing heat for the heating of buildings.

Another positive effect of storing water at high temperature instead of low temperature is the storage volume of water required to account for the needs of the building. This means that more temperature storage systems can be implemented, since the effective space required by the system is reduced. This also reduces the energy requirements of the system, since the pumps will need to pump less water.

Finally Sommer, (2007)[xiii] researched the effect of the soil characteristics of the efficiency of the ATES. He found that the higher temperature difference between the hot and cold storage, the higher the energy performance of the system, making HT-ATES more performant than L&M-ATES. This originates in the fact that dispersivity has a negative impact on the performance of an ATES. Dispersivity is an empirical factor quantifying how much a water particle will stray from the mean path. An effect of dispersivity is that the more water is injected, the more particles will deviate from the mean path. The goal of an ATES is to recover the water after injecting it. Because less water needs to be pumped in the aquifer with a HT-ATES, the dispersivity will affect less water flow. This diminishes the path length of water, hence a better performance.

2.2. Parameters influencing the efficiency of HT-ATES

In order predict the feasibility of a ATES Schout et al., (2014)[xiv] stated that a good method was to calculate the efficiency of the system. This recovery efficiency is defined as being the ratio between the recovered heat energy over the amount of energy injected with respect to ambient water temperature Ta, in other words: how much heat energy was lost during the storage process. The efficiency ε is described by Equation [1].

$$\varepsilon = \frac{Vp * Cw * (Tp - Ta)}{Vi * Cw * (Ti - Ta)} = \frac{Tp - Ta}{Ti - Ta} \quad [1]$$

where V refers to the volume of water injected or extracted [m3], Cw to the heat capacity of water [J/m3 K-1] the subscript p refers to production, i for injected. For Tp the average value of recovered water temperature will be taken. Everything reducing the recovery temperature will therefore influence the efficiency of the system negatively. At this moment HT-ATES systems have a recovery efficiency that is lower (50-90%) than that of L&M-ATES (75-95%) as showed Bloemendal et al., (2016).

Different factors influencing the efficiency of a HT-ATES are conduction, dispersion, horizontal and vertical permeability of the soil, hot water bubble recovery size, regional flow, water quality alterations, and finally free convection. We will briefly discuss these in order to get an overview of what could cause errors in our assumptions, but will focus mainly on free convection, since this is the focus of our study.

2.2.1. Heat conduction

The most obvious heat losses follow from conduction. Heat is transferred horizontally to the groundwater in the aquifer surrounding the hot water bubble, but also to the aquitards confining the aquifer vertically. The thickness of the aquifer, and thermal conductivity of surrounding layers can reduce this effect.

2.2.2. Dispersivity

Dispersivity deals with the unknown parameters of the soil that is being simulated. It refers to the amount of information that must be approximated in order to get a valid representation of groundwater flow. A high dispersivity means that a water particle will greatly deviate from the average water particle path. However, Schout et al., (2014) showed us in a sensitivity analysis of different negative impacts on the efficiency of HT-ATES that the effect of dispersivity is often negligible compared to that of free convection.

2.2.3. Horizontal and vertical hydraulic conductivity

Horizontal and vertical hydraulic conductivity, in correlation with injection volume have great impact on the efficiency of a thermal storage, as showed Schout et al., (2014). A great horizontal conductivity is positive for the efficiency, since it facilitates the injection and extraction of the water. Free convection occurs due to buoyancy forces. A great vertical conductivity facilitates flow in a vertical direction, therefore leading to more free convection losses.

2.2.4. Regional flow

Another factor of influence in the recovery efficiency of a HT-ATES can be regional flow. If there is a strong flow present a system of multiple wells will display different efficiencies, which can be explained by their relative positions to each other, and by their position compared to the flow. This was studied by Zeghici et al., (2015)[xv] . They modelled a situation where 5 monowells were placed in a square, with one in the middle of the four others, with a groundwater flow present. They concluded that the well in the centre position would obtain the high recovery efficiency. This can be explained by the fact that the central well suffers less heat loss due to the proximity of the other four wells, limiting the losses to the ambient groundwater. The well with the lowest recovery efficiency was upstreams of the groundwater flow, showing that when there is some flow present it will reduce the efficiency of a single well.

When dealing with High Temperature Storage, aquifers at great depth are often used. These layers usually show very little groundwater flow, meaning that in our case the effect can be neglected as showed Drijver, (2014)[xvi].

2.2.5. Chemical alteration

Chemical alteration of water remains one of the main problems of HT-ATES. It is however not in the scope of the study to discuss all of the consequences related to the chemical composition of water, but a quick overview of the problem will be discussed.
The rate at which water chemically alters can be defined by the rate of reaction. The rate of reaction (k) is exponentially dependant of the temperature increase of the groundwater, according to Hartog, (2011)[xvii] , as defined in Equation [2].

$$k = A \cdot e(-Ea/\ RT) \qquad [2]$$

With A being the reaction dependant prefactor, Ea the activation energy and R the gas constant. This means that as the temperature increases, reactions occur faster.
The main effect of this on the efficiency of a HT-ATES is the precipitation of calcium carbonate. The solubility of calcium carbonate in water decreases with increasing temperature, causing the precipitation around a 50 ℃ to 60 ℃. This problem is specific to HT-ATES, because the precipitation does not occur at the temperature of medium and low temperature ATES. The precipitations clogs up in the aquifer, causing the permeability to diminish, as stated by Drijver (2014). This makes the recovery of water more difficult, lowering the efficiency of the system. This can be counteracted by dissolving hydrochloric acid in the water, lowering the pH, which facilitates the dissolution of the precipitation in the groundwater. Care should be exerted when applying this method, since too much acid will negatively impact the quality of the groundwater. It is also possible to dissolute carbon dioxide. Brokx, (2016)[xviii], highlighted other chemical problems influencing the quality of the water when storing water at high temperature.

2.2.6. Free convection, or density driven flow

The most important factor of recovery losses with HT-ATES comes from density driven flow. It originates in the density difference between hot and cold water. Since the water that is stored is above 60 ℃, the hot water will be less dense than the cold water. Buoyancy forces will make the hot water flow to the top of the aquifer, while cold water will want to settle at the bottom of the aquifer. This tilts the thermal front, leading to heat losses originating from four principles, that were studied by Schout et al., (2016)[xix]. A visual representation of this principle is presented in Figure [5].

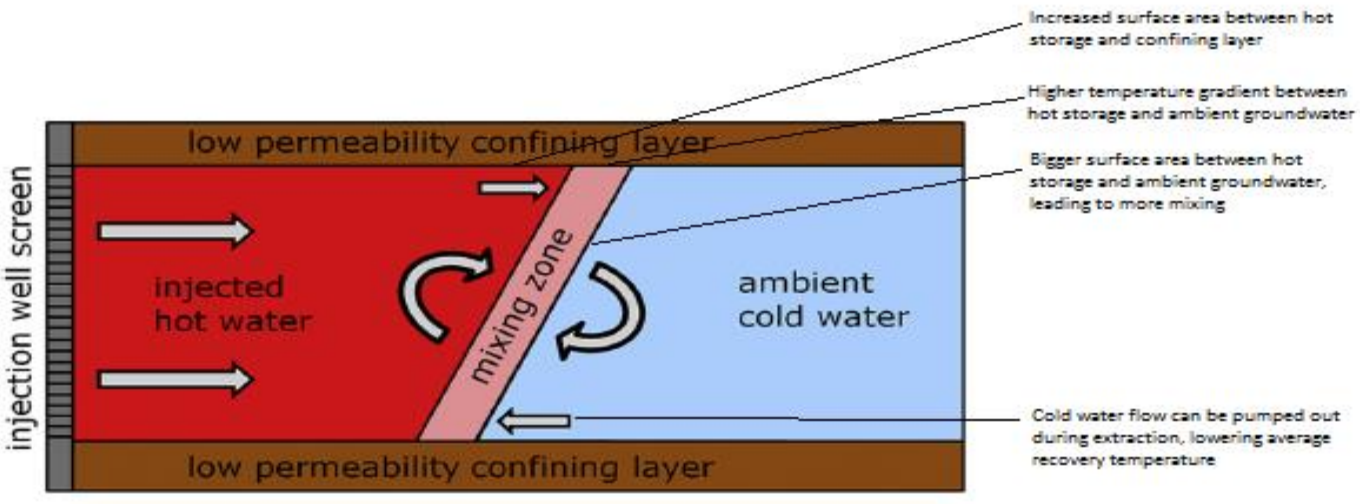

Figure 5 Illustration of the principle of density driven flow in an aquifer by Schout et al., (2016)

The first source of efficiency loss comes from the increased surface area between the hot water storage and the confining layer, leading to enhanced effective heat conduction. In the case of high temperature storage the temperature gradient is bigger than with LT-ATES. Conduction losses will therefore also be increased. The last effect of density driven flow during the storage issues from the bigger surface area between hot storage and ambient cold water. This comes from the tilting of the heat gradient.

The final effect of free convection on the efficiency comes into play during the recovery of the hot water bubble. Cold ambient water that flows towards the well during storage due to the density difference will also be recovered due to the initial velocity of the water, and its proximity to the well. This lowers the average recovery temperature of the system, and with this the efficiency.

In most reports concerning LT-ATES, it is stated that density driven flow doesn't affect the performance (Sommer, 2007). In the case of HT-ATES it accounts for most of the reduction in efficiency of the system, because the temperature difference between the hot water bubble and the surrounding groundwater is way larger. With the increased temperature difference comes a greater density difference, which will obviously lead to more losses related to free convection.

2.2.7. Heat Bubble

The tilting of the heat front brings another negative effect on the efficiency during the recovery phase. The combination of the initial flow of fresh water towards well, the tilted thermal front and the extraction creates a volume of water that cannot be recovered. A graphical representation of the adapted recovery efficiency was presented by Kimbler et al., (1975)[xx] in Figure [6]..Because of the geometry of the bubble after tilting and extraction of water, a conical volume of water cannot be recovered without mixing of fresh water. This effect was described by Ward et al., (2007)[xxi]. The volume of water that cannot be recovered is described by the shape of the conical water bubble, and is therefore depend on the initial radius to the 5% isochlor at the bottom of the interface r0,05, bottom [m].

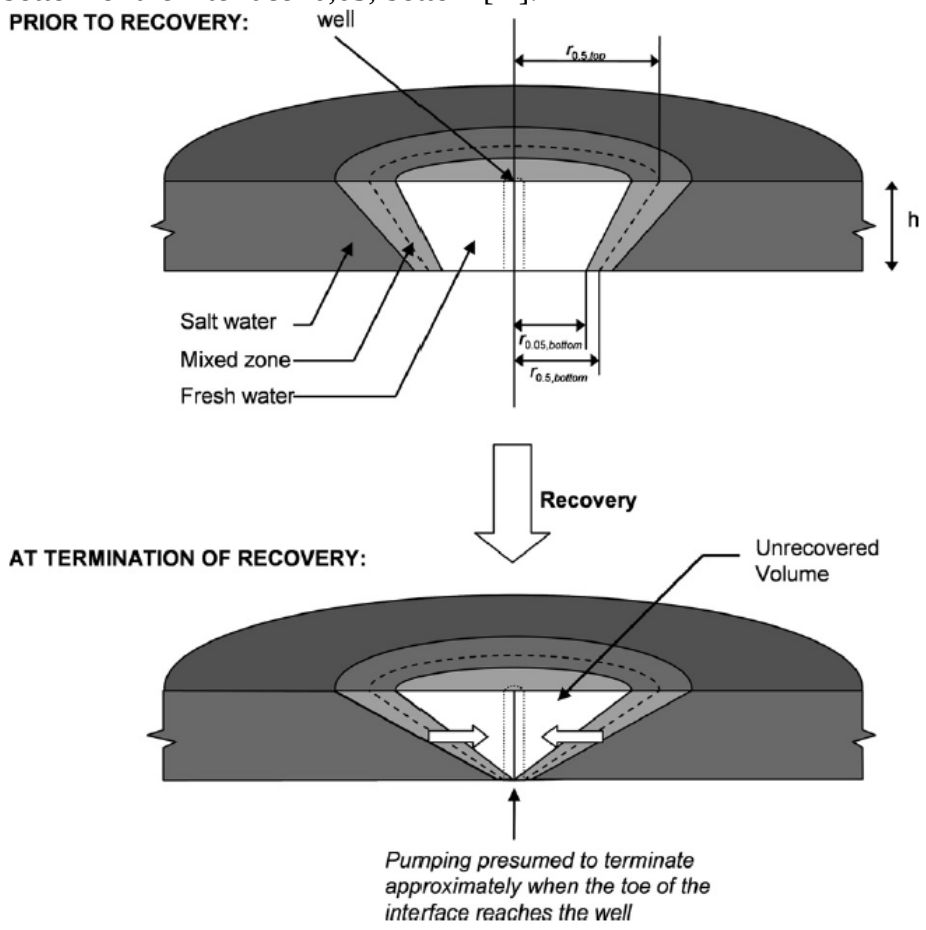

Figure 6 Representation of adapted recovery efficiency, by Kimbler et al. (1975)

The recoverability ratio R*, not to be confused with the net recovery efficiency of the system ε is defined as the volume of the unrecoverable water bubble volume to the total injected water. Ward et al., (2007) described it in Equation [3].

$$R* = \frac{\pi * H * \theta * (\mathrm{r0{,}05,bottom})^2}{Vi} \qquad [3]$$

With H the aquifer thickness [m], θ the porosity of the aquifer [-], and $r_{0,05,\,bottom}$ is the assumed position of the toe[m], Vi the injected water volume [m3].

2.2.8. Efficiency predictions of HT-ATES

Different approaches on estimation of losses related to density driven flow in HT-ATES are possible. The most commonly used method is a simulation, for example SEAWAT. This method enables to predict the temperature fluxes after a certain number of cycles. This method is an effective solution to predict long term effect of free convection. It is a better way of predicting analytically since the efficiency of an ATES tends to enhance after a number of cycli, as showed Lopik et al., (2016)[xxii]. This is because the effects influencing the efficiency mentioned above are being compensated after a number of times because they have already taken place in a cycle before.

Schout et al., (2014) also proposed an approach on estimating the recovery efficiency thanks to a modified Rayleigh's number, described in Equation [4]. It is based on the study of Gutierrez-Neri et al., (2011)[xxiii] who correlated the Rayleigh number Ra found by Nield and Bejan., (1999)[xxiv] to the recovery efficiency of an aquifer. They described the dimensionless number Ra as an indication of the relative strength of heat transfer through conduction and free convection. After coupling values from recovery efficiencies of temperature storages to their sensitivity analysis, they concluded that the injection volume Vi was missing in the recovery efficiency estimation. Also the vertical conductivity was replaced by √(kav*kah) since free convection is also related to the horizontal flow.

$$Ra^{*} = 1634 \cdot \frac{\rho \cdot H^{2,5} \cdot \sqrt{k_a^{v} \cdot k_a^{h}} \cdot \Delta T}{\mu \cdot \sqrt{V_i}} \qquad [4]$$

Where H [m] is the thickness of the aquifer, k_a^{v} and k_a^{h} [D] the respective vertical and horizontal permeability of the aquifer, μ [kg/(m*s)] is the dynamic viscosity of water, and Vi [m3]the injection volume.
They compared the value of Ra* to the modelled recovery efficiency, and found Equations [5] and [6].

$$When\ 10 < H < 60\ [m] \quad \varepsilon = \left(0.82 - \frac{1.70}{H^{1,2}}\right) \cdot e^{\left(-\frac{1,2}{H^{1.35}} + 2.2 \cdot 10^{-3}\right) \cdot Ra^{*}} \qquad [5]$$

$$When\ 60 < H < 200\ [m] \quad \varepsilon = \left(0.82 - \frac{1.70}{H^{1,2}}\right) \cdot e^{\left(\frac{-2,7}{H^{1,7}}\right) \cdot Ra^{*}} \qquad [6]$$

The relation between the recovery efficiency, the aquifer thickness and the modified Rayleigh's number is illustrated by Figure [7].

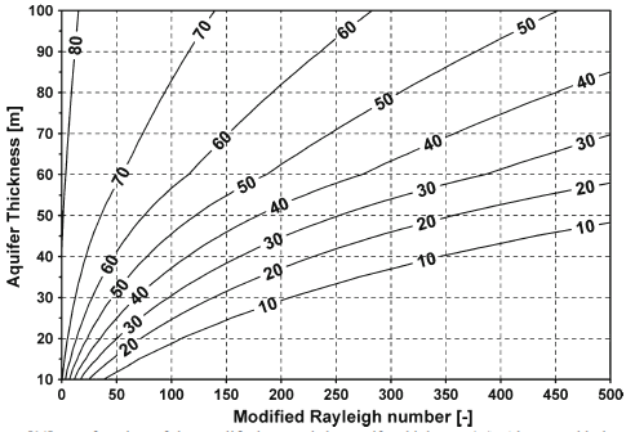

Figure 7 Relation between the aquifer thickness, modifies Rayleigh's number, and recovery efficiency (Schout et al., 2014)

The modified Rayleigh's number does not account for the density difference between the hot and cold water. Another way to relate the recovery efficiency to the density difference must therefore be found. A characteristic of free convection is the tilting of the thermal front. Hellstrom et al., (1979)[xxv] researched the

effect of density difference on the characteristic tilting time of the stored hot water with the ambient cold water. The expression of the time it takes for the hot water front to form an angle of 60 ˚with the vertical is presented in Equation [7]. This analytical method does not provide an estimation of the recovery temperature, making it impossible to calculate the final efficiency of a system. It does provide us with an order of magnitude of the effect of a density variation on a HT-ATES. A density difference reduction creates a longer tilting time. The amount of increase in tilting time will take provides us with an indication of the effect on the density driven flow.

$$t0 = \frac{H}{\sqrt{(kh * kv)}} * \frac{Ca}{Cw} * \frac{((\mu 0 + \mu 1)\pi^2)}{32G(\rho 0 - \rho 1)g} \quad [7]$$

Where t0 is the radial tilting time of the front to 60 ˚, kh and kv respectively horizontal and vertical permeability in m2, Ca and Cw the heat capacity of the aquifer in J/(m3K), μ the viscosity of water in kg/(ms), ρ the water density [kg/m3], G the Catalans constant, g the gravitational constant. The suffixes 0 and 1 refer to ambient and injected water respectively.

2.3. Effect of enhanced salt concentration on density driven flow

Since free convection is accountable for the biggest part of losses in an HT-ATES, Lopik et al., (2016) proposed a method to reduce the density difference between the stored hot water and ambient cold water. They goaled to achieve this by injecting water with a high concentration of dissolved salts in an aquifer. The conclusion of their study was that using water with magnified density was a good way to reduce the effect of free convection, even approaching the theoretical efficiency of such a system. We will try to use this principle in an aquifer at the TU Delft, by looking for water with a higher density due to higher salt content in a deeper aquifer layers. This deep aquifer will be used as cold water storage. The water with high density in the aquifer will be used for the hot storage, reducing the density difference between the hot storage water and the ambient groundwater.

2.3.1. Equations of State

In order to predict the effect of added salt to injected water in a HT-ATES, Lopik et al., (2016) modelled the groundwater temperature and salt concentration of a HT-ATES after 4 cycles in SEAWATv4. Equations of state were used to relate temperature and salt concentration to density and viscosity of the groundwater. Pressure was not taken into account in these equations because of the low compressibility of water. Also since the goal of our research is to compare to waters at the same pressure, compressibility could not play any role in the results obtained.

For the viscosity Equation [8] was used, first described by Voss (1984)[xxvi] .

$$\mu(C_S, T) = 2.394{\cdot}10^{-5}{\cdot}10^{\left(\frac{248.37}{T+133.15}\right)} + 1.923{\cdot}10^{-6}(C_S) \quad [8]$$

With μ being the dynamic fluid viscosity (kg/m day), T the temperature of the water (°C) and Cs is the salt concentration of the water (kg/m3).

For the density Equation[9] was used, as derived by Sharqawy et al., (2010)[xxvii] .

$$\rho(T,\ S) = \left(999.9 + 2.034{\cdot}10^{-2}T - 6.162{\cdot}10^{-3}T^2 + 2.261{\cdot}10^{-5}T^3 - 4.657{\cdot}10^{-8}T^4\right) + \left(802.0\frac{S}{1000} - 2.001\frac{S}{1000}T + 1.677{\cdot}10^{-2}\frac{S}{1000}T^2 - 3.060{\cdot}10^{-5}\frac{S}{1000}T^3 - 1.613{\cdot}10^{-5}\left(\frac{S}{1000}\right)^2 T^2\right) \quad [9]$$

where ρ is the fluid density (kg/m3) and S is the salinity of the water (g/kg).

2.3.2. Effect of density-difference compensation on efficiency

Lopik et al. (2016) modelled the temperature and salt concentration in a HT-ATES after 4 cycles. The results are shown in Figure [8]. In the left column the temperature contours over the depth are shown. On the right the salt concentration in the aquifer are shown. Situations (a) and (d) refer to the injection phase, (b) and (e) to the storage, (c) and (f) to the extraction phase. In the left column the plotted lines show the temperature contours of a standard HT-ATES reference case where no salt was added to counteract free convection.

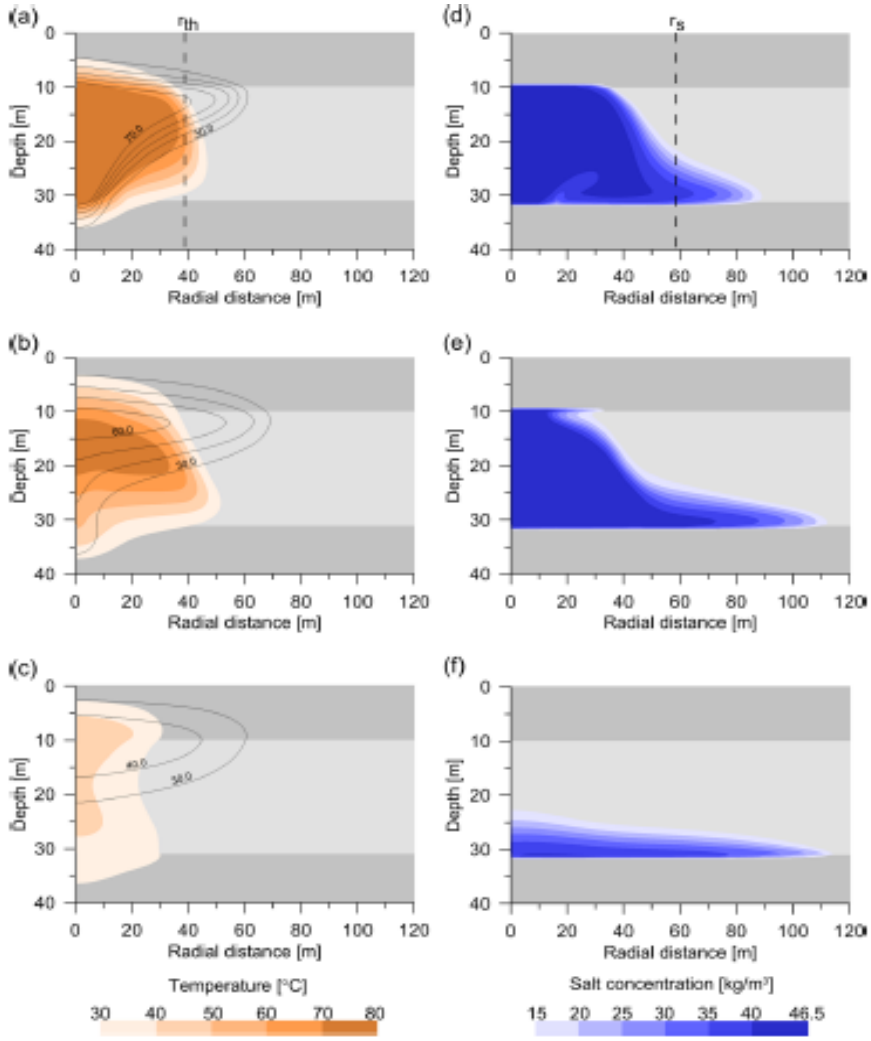

Figure 8 The effect of the reduced density difference between injection (a), storage (b) and extraction (c), Lopik et al. (2016)

During injection and storage, no more tilted front is present in the temperature distribution. Some salt accumulation is present at the bottom of the aquifer due to the conductive cooling of the stored water. In the extraction phase the recovery efficiency becomes higher. Free convection was counteracted, therefore cold ambient water flow towards the well was not present. This enhances the recovery temperature of the well, augmenting the system efficiency. Note should be taken of the accumulation of salt in the aquifer. The effect of the method is based on the lower salt concentration of the ambient water than the stored water. The salt accumulation in the aquifer will therefore overtime reduce the effect of added salt in the stored water.

A final effect of density-difference compensation is that because of the enhanced recovery temperature, significantly less water need to be pumped in order to fulfil the heat demand. This does not only reduce the energy cost of the pumps, but also the conductive losses in the aquifer.

2.3.3. System presentation

Our goal for the TU-Delft case study is to use water from a deep aquifer with a high salt content as hot storage water in a more shallow aquifer as a density-difference compensation. Because the plan is to use separate aquifers a monowell system seems to be the most logical option, like presented in Figure [3]. Adding another well for the cold storage would only increase the costs of drilling. A triplet could also have been chosen, however the focus of this study is to reduce the effect of free convection using water present on location with a high salt content. There would not be an advantage to studying that in the setup of a triplet. The goal of the system is to reduce the difference in densities $\Delta\rho$ between ρs and ρa, where a refers to the ambient water of the storage layer and s refers to the stored water.

3. Estimation of groundwater density in Delft

In order to predict the density of groundwater Equation [9] was used. In this model the density of water is dependent on temperature [C ˚] and salinity [g/kg]. For the temperature of the water the geothermal gradient of Delft will be followed. For the salt concentrations data provided by Dinoloket will be used for the first 150m. For deeper layers assumptions of the salt gradient will be made based on the salt concentration of water from deep geothermal wells.

3.1. Geothermal heat gradient

The temperature of the soil is of importance for the prediction of the density of the water in the ground. Edelman (2004)[xxviii] created a map of geothermal gradients in the Netherlands based on a series of measurements between 1977 and 1983performed by TNO. These are presented in Appendix [2], with the geothermal gradient in Delft. The first 100m are assumed to be at constant temperature of 13 C ˚, since this region is subjected to seasonal temperature variations. From there the geothermal gradient linearly enhances the temperature with depth, due to heat present in the core of the Earth. This gradient is strongly dependant on the location. In the Netherlands it can vary from 11 C ˚/km to 35 C ˚/km, with an average value of 24 C ˚/km. In Delft we assume a value of 20 C ˚/km, based on the temperature gradients of surrounding locations. The graphical representation of the Geothermal gradient in Delft is shown in Figure [9].

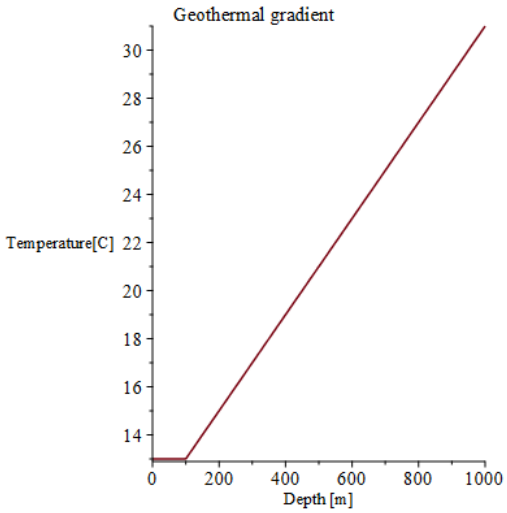

Figure 9 Geothermal gradient of Delft

3.2. Salt concentration gradient

3.2.1. Salt concentration variation with depth until 150m

The salt concentration in the groundwater under Delft can be estimated based on water composition measurements provided by TNO. They offer a great range of information concerning the composition of the soil and groundwater in the Netherlands through the platform Dinoloket. The 3 deepest wells in the surroundings of Delft were used as a basis to find the salt gradient in the shallow layers of the soil. In appendix D the location of the 3 wells B37F0104, B37B0181 and B37E0382 is shown, with the salt concentration, water density and depth of each measurement. These wells provided [CL-] and [Na+] concentrations over a depth varying from -19,75 to -124,5m .The location of the wells, and the data of the water composition are presented in Appendix [3]. The salinity is expressed in Equation [10]. Combination of Equation [9] with Equation [10], and iterating permitted to find the water density and salinity at different depth. A base value of ρ_W= 1000+[Cl-, Na+]/1000 was chosen.

$$S = \frac{[Cl-] + [Na+]}{\rho w} \qquad [10]$$

With [Cl-] and [Na+] concentration of chloride and nitrate in [g/m3], ρW the density of water in [kg/m3], and S the salinity in [g/kg]. The results are presented in Figure [10].

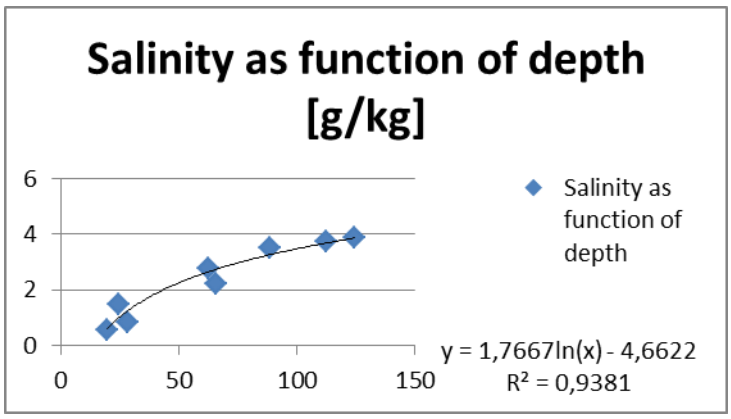

Figuur 10 Salinity as function of depth based on Dinoloket data

A regression line through the data points showed a logarithmic tendency in the first 150m depth of the soil. The regression equation over a depth varying from 0-150m is presented in Equation [11].

$$S = 1{,}7667 * \ln(D) - 4{,}6622 \quad [11]$$

With S the salinity in [g/kg], D the depth in [m].

3.2.2. Salt gradient estimation from 150m to 600m

J. Grifioen (2015)[xxix] studied the composition of deep groundwater in the Netherlands for TNO. The data of the chloride concentration from the wells in presented in Appendix [4]. A conclusion drawn from the well data was that the salt gradient of groundwater is entirely dependent on the location of the well. No relation can be drawn as to the exact salt gradient without sample data from the location. This is because the salt concentration also varies depending on the ground layer. Assumptions will therefore need to be made concerning the salt gradient, since no data of deep groundwater of Delft is accessible.

JJ. de Vries (2007)[xxx] also studied the salt concentration of the groundwater in deep layers. In some measurements from the Haarlemmermeer polder a linear evolution of salt concentration seems to appear. A linear salt gradient will therefore be assumed, due to the lack of salt concentration data of deep groundwater in Delft. His study also provided a value for a salt concentration of ground water at 840 m of 18400 [mg/L], which we will use for finding a regression of the salt gradient.

The composition of water in deep geothermal wells can serve as a basis to try to linearize the salt gradient. N. Hartog (2016)[xxxi] researched the salt content in deep geothermal wells in the Netherlands. The data from [Cl-] and [Na+] concentrations are presented in Appendix [4]. The depth of each well remains unknown. Geothermal wells in the Netherlands typically have depth varying from 1500 m to 3000m. The well with the lowest salinity has a concentration of 52500 [mg/L]. An under boundary for the salt gradient can therefore be found at 17[mg/L m-1] by assuming that this was placed at 300m depth. The well with the highest salinity has a concentration of 220000 [mg/L]. Since we assumed that the salt gradient was linear we can assume that this well was at a depth of 3000m. This provides an upper boundary for the salt gradient of 77[mg/L m-1]. As reference case we will assume the lowest salinity was found at a depth of 1500m. This provides a salt gradient of 35[mg/L m-1]. For the linearization the data from Dinoloket, the concentration of Limburg from JJ. de Vries (2007), and the data from N. Hartog (2016) were used. The 3 cases mentioned above are presented in Appendix [5]

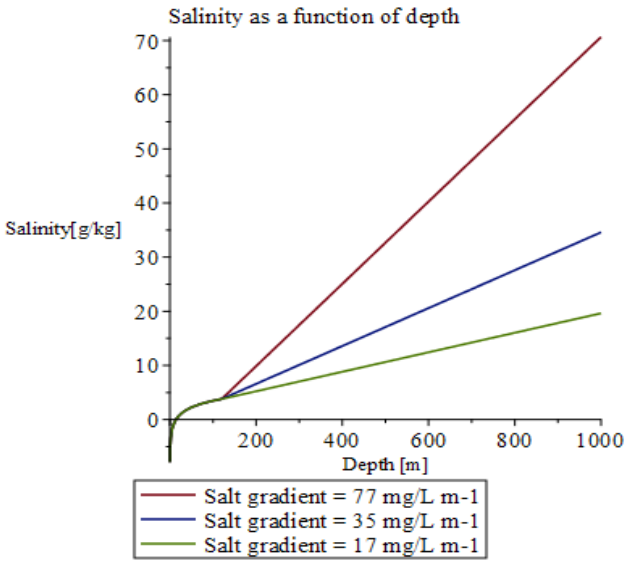

Figuur 11 Salinity estimation as function of depth

Combination of concentrations from 0-150m and 150-600m provides us with an estimation of groundwater salinity as a function of depth presented in Figure [11]. The green line shows the under boundary, blue the reference case and red the upper boundary. Note should be taken that the lower boundary fits best to the data collected from Dinoloket, it would therefore seem that the lower boundary come closest to the real situation in Delft. The reference case also seems acceptable. The upper boundary does not fit well to the first 150m salt concentration.

3.2.3. Groundwater density as a function of depth and geothermal gradient

Combining the geothermal gradient with the salt gradient into the Equation [8] returns the density as function of depth. As for the salinity it looks like the under boundary is most representative of the reality.

The density is mostly dependent on the linear salt concentration, and seems to be less affected by the temperature gradient. This is because the depth of the storage is relatively low, therefore the temperature gradient does not greatly influence the temperature of the ambient groundwater. We can note that for the scope of study the density enhances with depth. This means that density-difference compensation is possible.

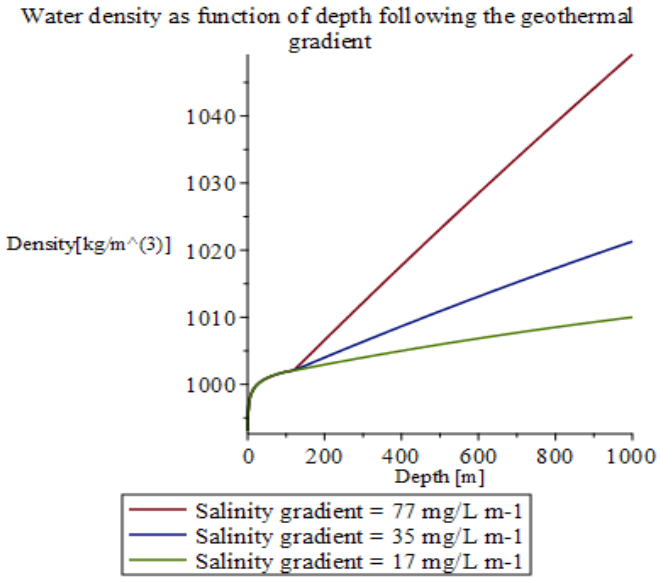

Figuur 12 Density as a function of depth for 3 different salinity gradients

3.2.4. Groundwater density as a function of depth and fixed storage temperature of 60°C

The goal of the system is to reduce the density difference between the hot storage water and the ambient groundwater. In the previous paragraph we showed the density dependency of groundwater on the geothermal gradient and salt content. The density of groundwater at storage temperature is shown in Figure [13].

For every salt gradient we note that the density enhances with depth. This means that the bigger the depth difference between hot and cold storage aquifers will be, the smaller the density difference between stored water and ambient groundwater.

In the next chapter we will couple our density results for ambient water and storage water with the soil layers present under the TU Delft, in order to predict the density difference before and after density-difference compensation.

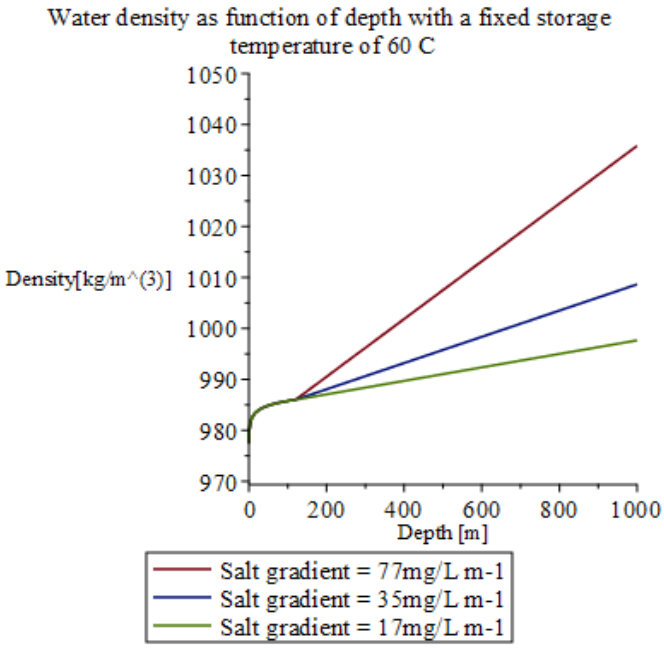

Figure 13 Density as function of depth with a fixed storage temperature of 60 C

4. Suitable layer combination in Delft

In order to evaluate the efficiency of compensating density-difference by using water from a deep aquifer as storage in a more shallow aquifer, the subsurface of the TU Delft will be used as a base. Hacking T., (2017) evaluated suitability of the layers in the subsurface for HT-ATES. He concluded that three layers were possibly suitable for HT-ATES, under the condition that further research is carried out concerning the vertical and horizontal hydraulic conductivity of the layer. In the next paragraph the different layers will be presented. Finally the water densities in each layer will be coupled to the storage temperature density of the deepest layer in order to predict the density-difference compensation effectiveness. For the salt gradient the reference case will be used to determine the densities.

4.1. Aquifer possibilities for HT-ATES

4.1.1. Maassluis formation

The first possible aquifer for the storage is the top part of the Maassluis formation found thanks to the Dinoloket data. It starts at a depth of 160m , with a thickness of 20m. Hacking, T. (2017) found that the aquifer was suitable due to the high horizontal permeability of (10 <kh <100 m/d) and low vertical permeability of (0.001 <kv<1 m/d). The layer is described as having medium sized grains. In Chapter 3 was concluded that the density of water increased with depth. In order to increase the density-difference compensation the layer with the lowest density should be used as storage. Since this layer is the most shallow possible storage layer it is the best storage layer.

4.1.2. Berg Sand

The second layer Hacking, T (2017) found to possibly suitable for HT-ATES is the Berg Sand layer. It is situated at the bottom of the Breda formation, at a depth of 420m, with a thickness of 20m. Further research should be carried out as to the presence of this layer on the TU Delft. It was found in a well in Pijnacker, but not in the possibly outdated nomenclature of the TU-Delft. Also, further research should be carried out as to the porosity and hydraulic conductivity of this layer.
In the goal of our study this layer will be studied as cold storage, and will be compared with the deeper laying Texel Member. Since the stored cold water will not have a great density difference with the ambient water, the horizontal hydraulic conductivity is of more importance than the vertical conductivity.

4.1.3. Texel Greensand member

The final layer that was established as possibly suitable for cold storage is the Texel Greensand member. At the location of the TU-Delft it is located at a depth of 560m, with a thickness of 20m. It is mostly composed of sand-stone, with small layers with low hydraulic conductivity, making it interesting for HT-ATES. No information on the permeability at the location is known. In Pijnacker the layer was located at 955 m and showed permeability's around 15 mD. The pressure in the more shallow location of the TU-Delft is much lower, which could lower this permeability. For this layer further research should also be carried out.

4.2. Estimation of final density difference in storage aquifer

The goal of this study is to evaluate the effect of density-difference compensation. Water from a deep aquifer with a high density due to a high salt concentration will be used as high temperature storage water for a more shallow aquifer at the TU-Delft location. In the previous chapters the density of groundwater was estimated, and the aquifers in Delft suitable for HT-ATES have been presented.

The conditions for this HT-ATES system is that it uses water from the Berg sand layer or the Texel Greensand member as hot storage water in the top of the Maassluis formation. For further indication of

density suffixes M, B and T will be used to reference to layers of Maassluis, Berg and Texel. Temperatures will as before be noted Ta of ambient temperature and Ts for storage. Water originating from the Maassluis formation, at ambient temperature will for example be referred to as ρM(Ta). Water originating from Berg sand, and injected into the Maassluis formation at hot storage temperature will be noted ρB(Ts), with ρ in [kg/m3], and T in ℃.

Now that the different densities have been defined the density difference compensation in the Maassluis formation can be estimated. The initial density difference in the aquifer Δρi is the difference in density between the hot storage in the aquifer and the ambient groundwater, therefore Δρi can be expressed as in Equation [11].

$$\Delta\rho i = \rho M(Ta) - \rho M(Ts) \quad [11]$$

The final density difference after extraction of water from a deeper layer X and stored in the Maassluis Δρf can be expressed by Equation [12].

$$\Delta\rho f = \rho M(Ta) - \rho X(Ts) \quad [12]$$

The density difference compensation is the difference between the initial density difference and the density difference after the compensating effect. In this case we obtain by combining Equation [11] and [12] the expression of the net density difference reduction Δρi-Δρf and the density difference compensation percentage DDC [%] can be defined in Equation [13] and [14].

$$\Delta\rho i - \Delta\rho f = \rho X(Ts) - \rho M(Ts) \quad [13]$$

$$DDC = \frac{\Delta\rho i - \Delta\rho f}{\Delta\rho i} * 100 \quad [14]$$

Results of different density different compensation by using water from Berg Sand layer or Texel Greensand member as storage in the Maassluis formation are presented in Tabel [1]. The reference case salt gradient of 35mg/L was followed. Results for other gradients are presented in Appendix [6]. Injection temperature is set at 60 ℃. Note that no density compensation is present in the Maassluis formation, since it is used as reference storage layer. The original density difference is Δρi =16 kg/m3.

	Depth [m]	Width [m]	Ambient density [kg/m3]	Storage Density [kg/m3]	Δρi-Δρf [kg/m3]	DDC [%]
Maassluis Formation	160	20	1003,29	987,30	-	-
Berg Sand	420	20	1009,13	993,73	6,44	40,26
Texel Greensand	560	20	1012,25	997,34	10,04	62,80

Table 1 Calculation of density difference compensation by using water from Berg sand or Texel Greensand as storage in the Maassluis formation

A density difference compensation Δρi-Δρf = 10.04 kg/m3, can be won by extracting water from the Texel Member for storage in the Maassluis formation. This is equivalent to a reduction of 40% of density difference. In order to fully compensate density the cold storage should be placed at 790m depth. A visual representation of the density difference is provided in Figure [X]. Crosses show density of the Maassluis formation, triangles the Berg Sand and circles the Texel Greensand member. Blue colours refer to ambient groundwater temperatures, while red colours show the densities at storage temperature of 60 ℃. As was predicted before it is clear from the contours that minimum density difference is obtained by storing hot water from the Texel layer in the Maassluis formation.

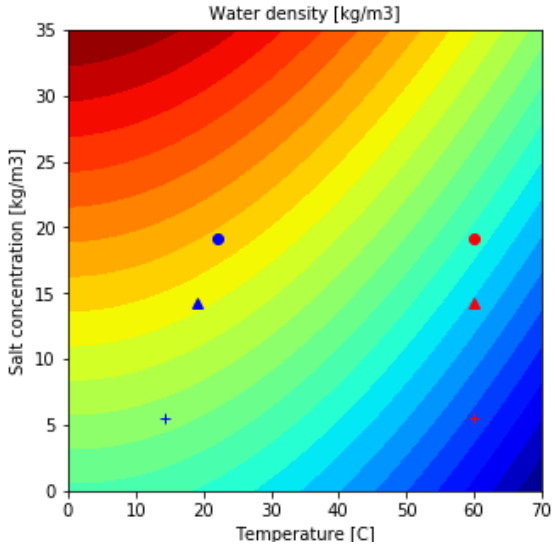

Figure 14 Water denisty contour, with density of different aquifer and water temperatures

5. Efficiency improvement

The final step of this research is to estimate the tilting time before and after density-difference compensation. First the different parameters influencing the tilting time will be presented before calculating the tilting time improvements. After that the mixed convection parameter will be discussed. This will permit us to discuss the effect of the compensation during injection and extraction. Finally salt accumulation in the aquifer after a large number of cycles will be presented, showing that the efficiency of the compensation will diminish over time.

5.1. Tilting time estimation

5.1.1. Tilting time parameters

In order to predict the efficiency of density difference compensation the tilting time of the heat front to 60˚to the vertical can be assessed, presented in Equation [7]. Parameters of the soil influencing the tilting time are the width of the aquifer, vertical and horizontal hydraulic conductivity. A wider aquifer will enhance the tilting time. Similarly a high combined vertical and horizontal hydraulic conductivity decrease the tilting time. A high horizontal conductivity is positive for the efficiency of a system as was explained in Chapter 2, therefore a low vertical conductivity is preferred to reduce the tilting time, and with that reduce the effect of free convection.
Viscosity measures the resistance of a fluid to deformations. A high viscosity will therefore slow the free convection process. This increases the tilting time. The method of density difference compensation is based on an enhanced salt concentration of the injection fluid. From Equation [8] we note that a high salt concentration increases the viscosity of a fluid. This means that the density difference compensation will both diminish the tilting time through the density difference reduction and the augmentation of the viscosity of the injected water.

5.1.2. Effect of system on tilting time

The tilting time of the previously discussed combination of aquifers can now be estimated. Some assumptions concerning the hydraulic conductivity of the Maassluis formation need to be made. Hacking (2017) found that the Maassluis formation possessed hydraulic conductivities in the ranges (10 <kh <100m/d) and (0.001 <kv <1m/d). In order to be able to implement them in the tilting time equation they need to be converted in mD. This was described by Duggal and Son (1996)[xxxii] . They stated that at room temperature and under hydrostatic pressure 1/md was equivalent to 8,31*10-13 mD. Note should be taken that HT-ATES do not operate at room temperature. This may cause some errors.
3 different combinations of hydraulic conductivities will be considered: A reference case of average values will be presented in the report, while upper and lower boundaries for tilting time will be given in Appendix [6]. First a high horizontal conductivity and vertical conductivity will provide an under boundary for the efficiency of the system. As reference case the average values of the range will be used. For the upper boundary a low conductivity will be chosen. The results for the reference case are presented in Table [2], the results for other combination can be found in Appendix [6].
For the heat capacity Cw and Ca of water and of the soil the same values as Lopik et al., (2016) were used.

	Depth [m]	Width [m]	Tilting time (d)	Tilting time increase (d)	Time increase [%]
Maassluis Formation	160	20	2,32	0,00	0
Berg Sand	420	20	3,91	1,58	68,13
Texel Greensand	560	20	6,29	3,97	170,74

Table 2 Tilting time of thermal front in the Maassluis formation with storage water from different layers

The original tilting time of the thermal front of the reference case in the Maassluis formation was found to be 2 days. When compensating the density difference in the Maassluis formation with water originating from the Berg Sand member this time increase by 68%. When using water originating from the Texel Greensand it increases with 170%. The tilting time drastically starts increasing when approaching the optimal depth of 790m, as is shown in Appendix [6].

The range of hydraulic conductivity greatly influences the tilting time. For the same salt gradient the tilting time can vary from under a day to more than 300. It is therefore of critical importance to get a better estimation of the real hydraulic conductivity present in the Maassluis formation.

If further investigations concerning the actual salt gradient is done, it should therefore need to be investigated if an aquifer is present closely to the optimal density difference compensation depth. If full compensation is possible, Lopik et al., (2016) modelled that a recovery increase $\Delta\varepsilon=0.2$ is possible. In the case of the Texel Greensand the density-difference compensation will have a lot less effect on the efficiency, since the tilting time is significantly more affected when density differences are extremely small. In case of a high salt gradient the optimal layer for density difference compensation can be in the relatively shallow depth we have investigated.

5.2. Forced or free convection

5.2.1. Mixed convection parameter

In a system with density difference and with a flow present it is important to assess whether the flow will be forced (due to a hydraulic gradient induced by the pump) or free (due to density-driven flow) in nature. Ward et al., (2007) proposed to predict the nature of the flow based on a mixed convection ratio M. This ratio the ratio between the theoretical flow velocity that are forced in nature to the convective ones. It is expressed in Equation [15]. M>>1 would refer to a flow dominated by density difference. M≈1 shows a balanced flow, while M<<1 shows a pump induced dominant flow. A visual representation of this is shown in Figure [15].

$$M = \frac{vfree}{vforced} \qquad [15]$$

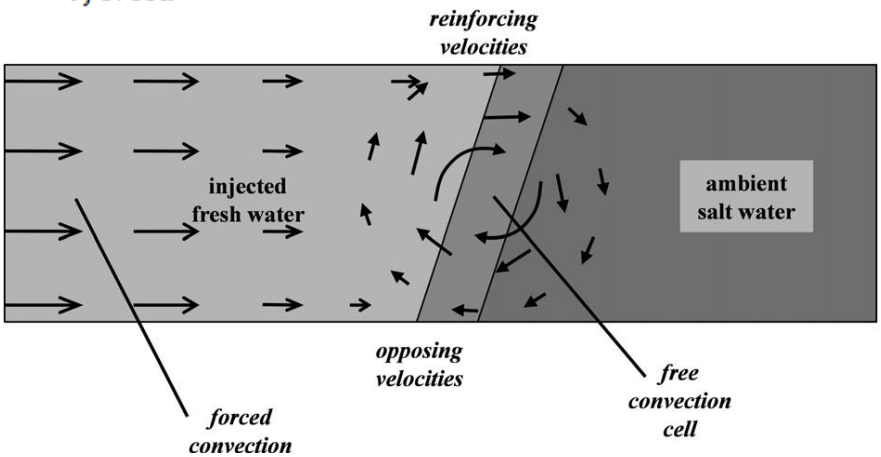

Figure 15 Visual representation of dominance of free or forced convection by Ward et al (2007)

The conclusion was that during storage free convection will obviously dominate, since no pump induced flow is present in the layer. It could also be noted that quite often during injection or extraction M<0.1, which indicates a pump forced convective regime. However in some cases tilting was showed to occur during injection or extraction, which indicates further research on the M parameter needs to be carried out for this density difference compensation combination in the Maassluis formation.

5.2.2. Free convection during injection and extraction leading to salt accumulation

In the case of density difference compensation an another parameter should be taken into account when studying the theoretical speed of water induced by free convection. The aquifer soil has a significantly higher heat conductivity than the surrounding groundwater. This means that as water is being injected, heat will be delivered from the storage water to the soil, resulting in the retardation of the thermal front compared to the water front.

The retardation of the thermal front during injection results in water front with high salt concentration and ambient groundwater temperature. The situation for our reference case is represented in Figure [16]. The 3 different water densities that will occur during injection and extraction can be described such that:
ρs(Ts) <ρa(Ta) <ρs(Ta)
In the reference case this leads to a density difference during injection and extraction of 10 kg/m3. This is still less than the original 16 kg/m3 density different present in the Maassluis formation, but still result in significant buoyancy forces. If the result of the mixed convection parameter leads to a value of M that is close to 1 these losses should be taken into account when studying the efficiency improvement of density difference compensation.

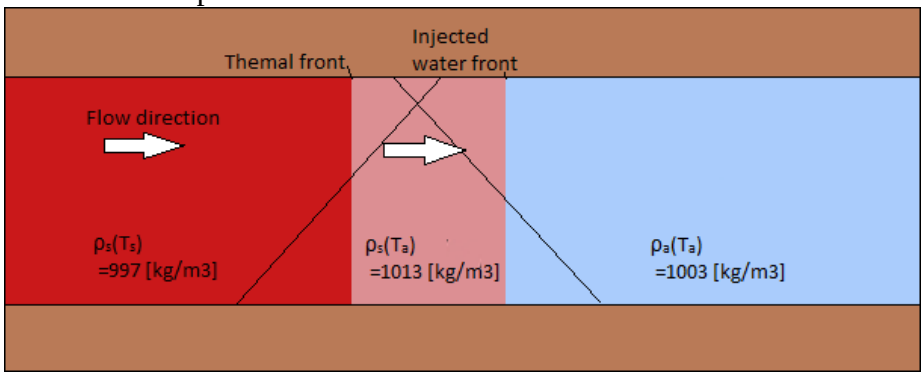

Figuur 16 Schematical representation of retardation of thermal front during injection, and possible effect on tilting of waterfront in the reference case

If free convection driving forces are significant, and convection cells around the two tilting fronts will form. Over time this might influence the salt recovery efficiency of the system. The salt that cannot be recovered accumulates in the aquifer. This eventually results in the blurring of the different density fronts. After an increased number of cycles the accumulation of salts will therefore reduce the effect of density difference compensation. A model taking salt losses into consideration is therefore needed in order to conclude on the long term efficiency of a density difference compensation in the case of a mixed convective regime.

6. Discussion

In order to assess the potential for density difference compensation on the TU Delft, aquifer locations that were concluded possibly suited for thermal storage were assumed to be suitable. The hydraulic conductivity is of great importance for the final tilting time. Further research concerning the aquifer properties should be carried out in order to provide good estimations of horizontal and vertical hydraulic conductivity. If it is found that the hydraulic conductivities are high density difference compensation will be less effective.

Little information concerning the salt gradient in deep soil layers was found. This led to a large estimation of the range of possible salt gradients. The magnitude of the salt gradient is of great importance to the density difference compensation. It also influences the optimal design depth for density-difference compensation. The proximity of the compensating layer to the optimal compensation depth was shown to be the most influential parameter in the estimation of losses due to free convection. No valid conclusion will therefore be able to be made until the salt gradient on location is researched.

Salt accumulation over time was shown to influence the effect of density-difference compensation after a great number of cycles. The effect of long term density-difference compensation on the salt accumulation in the Maassluis formation aquifer should be modelled in order to estimate the magnitude of this accumulation, and what effect this will have on the recovery temperature of the HT-ATES.

A study of the Mixed convection parameter should also be carried out. This is to assess whether the flow of water from the well is of forced or free convection dominance. If free convection turns out to be influential during injection or extraction the salt accumulation in the aquifer over time will also need to be studied to provide a long term estimation of the efficiency of this density-difference compensating system.

Finally a cost study needs to be made. A final estimation of the recovery efficiency in the case of density difference compensation modelled according to the points mentioned above would provide a base for a cost-efficiency study. The price of drilling of a well to a depth exceeding 500 m instead of 160m should be compared to the theoretical efficiency improvement from the density-difference compensation.

7. Conclusion

The goal of this thesis was to evaluate the effect of density-difference compensation on the tilting time of the thermal front in a HT-ATES on the TU-Delft. The density-difference compensation method was based on using water with a high salt concentration from a deeper aquifer (which is used as cold storage) as storage water in a more shallow aquifer.

The effect of the compensation was found to be entirely dependent on the salt gradient assumed, and the soil properties of the aquifer. A great improvement of the tilting time of the thermal front could be achieved if the salt gradient provided a final density difference that was very small. The effect decreases drastically when the cold storage aquifer is situated further away from the optimal density-different compensation depth. It is therefore critical to assess this depth depending on the actual salt gradient present in the subsurface of the TU-Delft

Summary

The first part of this thesis consisted of determining the various parameters influencing the efficiency of a system. Free convection was found to be originating in the density-difference between stored water at high temperature and ambient groundwater. The tilting time of the thermal front with an angle of 60 ° to the vertical was presented as an estimation of losses related to free convection.

A density-difference compensation method was presented. It is based on a high salt concentration of injected water, originating from a deeper laying aquifer that will be used as cold storage. In order to estimate the effect of such compensation the density of water in the soil needed to be determined. The density of groundwater was found to be dependent on its temperature and salt gradient
The first step was determining the geothermal gradient in Delft. It was found to be at 20 °C/km, starting at a depth of 100m.
A stepwise salt gradient estimation was provided. For the shallow subsurface (<150m) data from Dinoloket was used to determine the salinity of groundwater. For deeper layers estimation were made base on salt concentration of geothermal wells at great depth, due to the lack of data of the subsurface in Delft. This provided a salt gradient range of 17 mg/L to 77mg/L, with a reference value of 35 mg/L.

The layers that might be suitable for the HT-ATES in Delft were based on Hacking (2017). For the storage layer the top of the Maassluis formation (depth 160m) was chosen. The storage water originating from the Berg Sand formation (depth 420m) was compared to water from Texel Greensand Member (depth 560m). For different aquifer properties and salt gradients the tilting time improvement thanks to the density difference compensation were presented.

A density-difference compensation of 60% was estimated in the reference case of the study, by using water from the Texel member as storage in the Maassluis formation. Increase in tilting time of 170% was estimated for this reference case. The tilting time can be increased dramatically if the deep cold storage is situated close to the optimal density-difference compensation depth. It is therefore critical to find this depth based on the actual salt gradient present on the TU-Delft location. The tilting time was also found to be strongly dependent on the aquifer hydraulic conductivity. Small conductivities lead to high tilting times. Opposing, high conductivities induce a free convection dominant flow, leading to large efficiency losses.

Salt accumulation in the aquifer was found to be possibly increased with this density-difference compensation method, due to free convection during injection and extraction of storage water. In order to predict this the mixed-convection ratio M will need to be determined in a future study. All these effects should finally be modelled in order to estimate a recovery temperature of the HT-ATES. Salt accumulation over time should also be modelled for the long term effect of the compensation.

8. Appendix

Appendix [1] Functionning of a monowell (Zeghici et al, 2015)

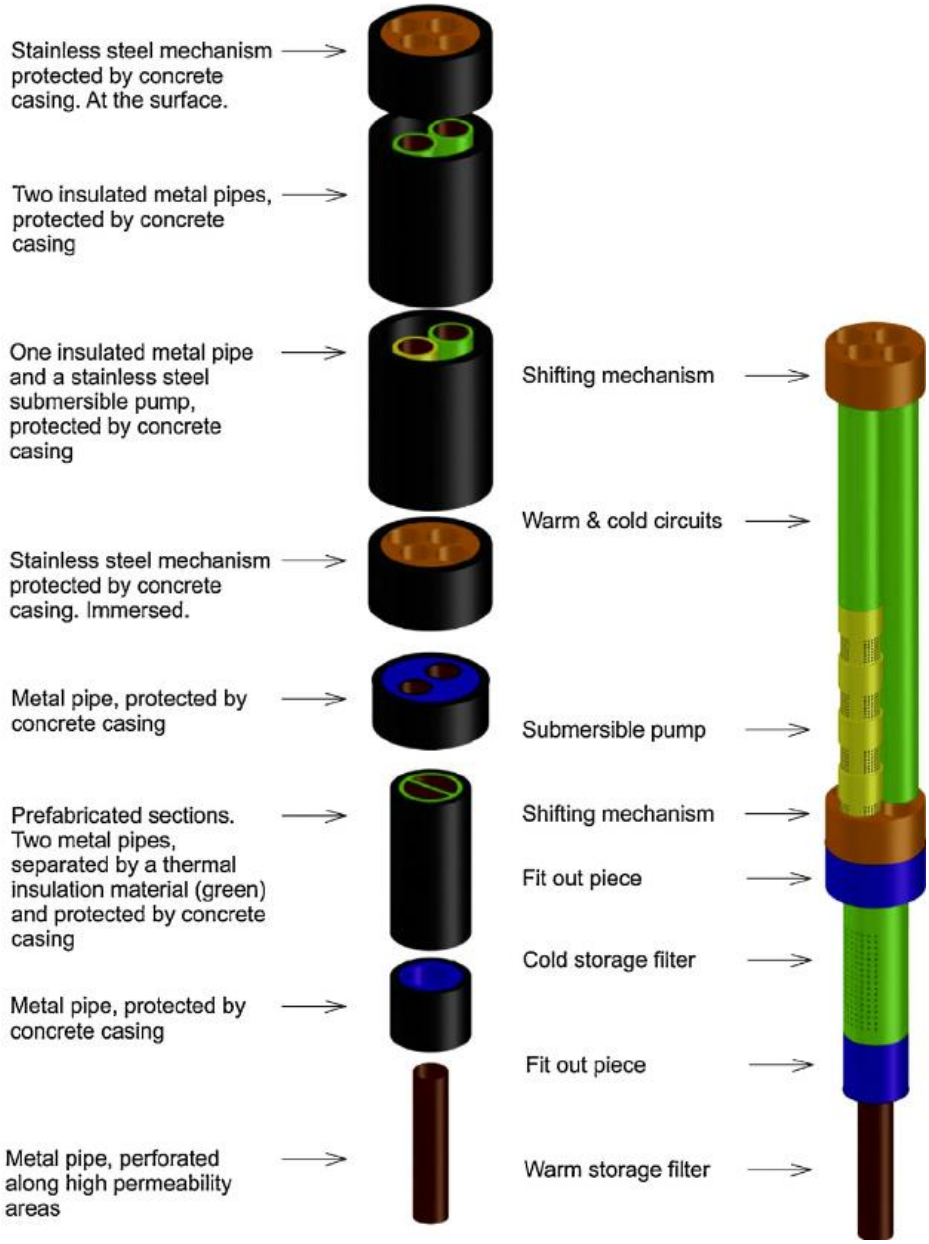

Appendix [2] Geothermal heat gradient in the Netherland (April 2004, D Edelman)

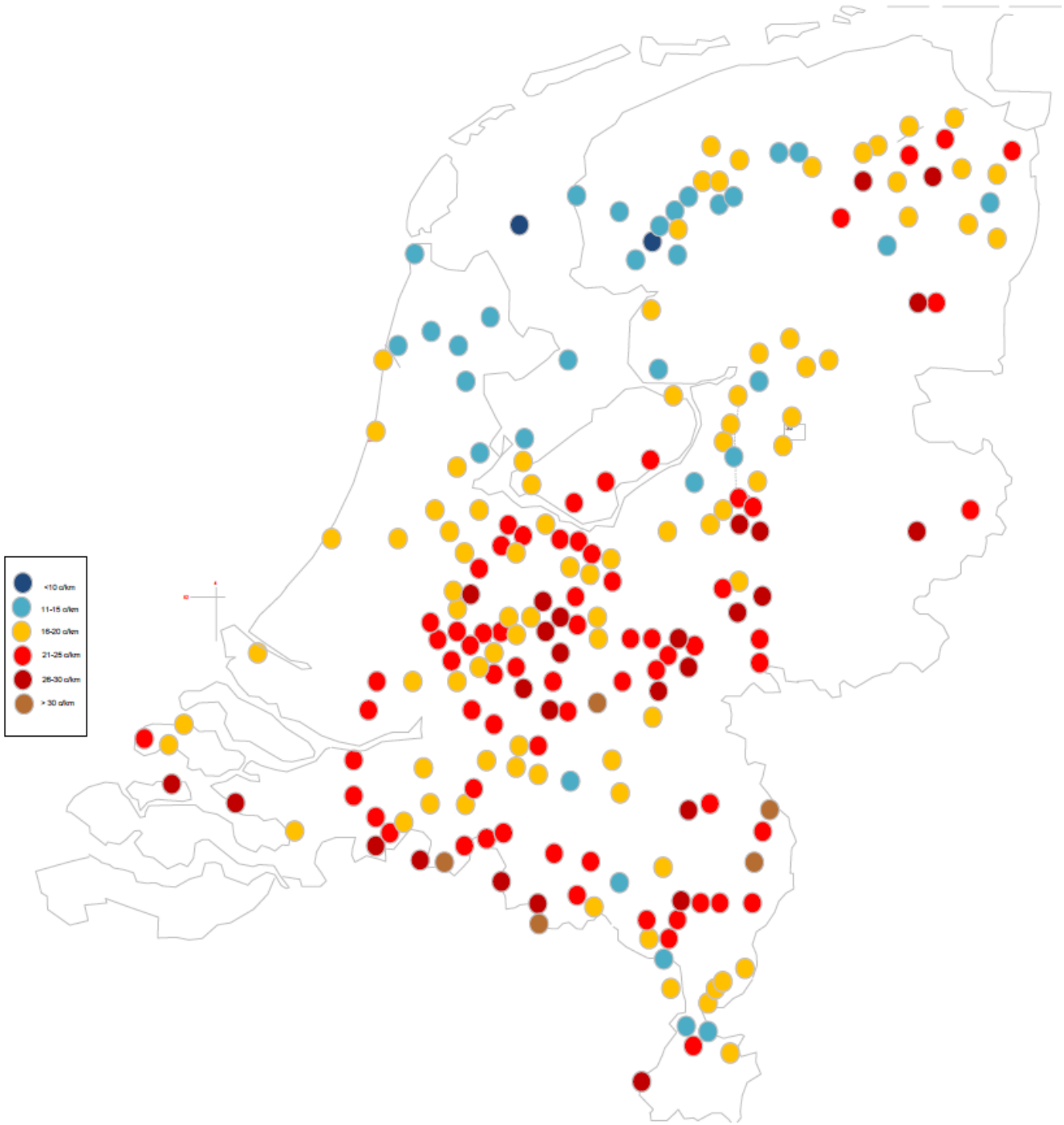

Appendix [3] Dinoloket water data presentation and area of study for possible wells

Monsteropname code	Diepte opname [m]	Temperatuur [C]	[Cl-]+[Na+] [g/m3]	S [g/kg]	ρ [kg/m3]
B37F0104	19,75	13,28	568	0,57	999,58
	28,5	14,31	849,84	0,85	999,65
	65,5	13,7	2235,11	2,23	1000,82
	112,37	9,87	3754,66	3,75	1002,46
	124,5	8,87	3871,51	3,86	1002,64
B37B0181	88,65	18	3510	3,51	1001,10
B37E0382	24,5	18	1486	1,49	999,54
	62,5	18	2775	2,77	1000,54

Tabel 3 Dinoloket water compensation data

Appendix [4] Chloride concentration in deep groundwater layers in different regions of the Netherlands, and deep geothermal wells in the Netherlands

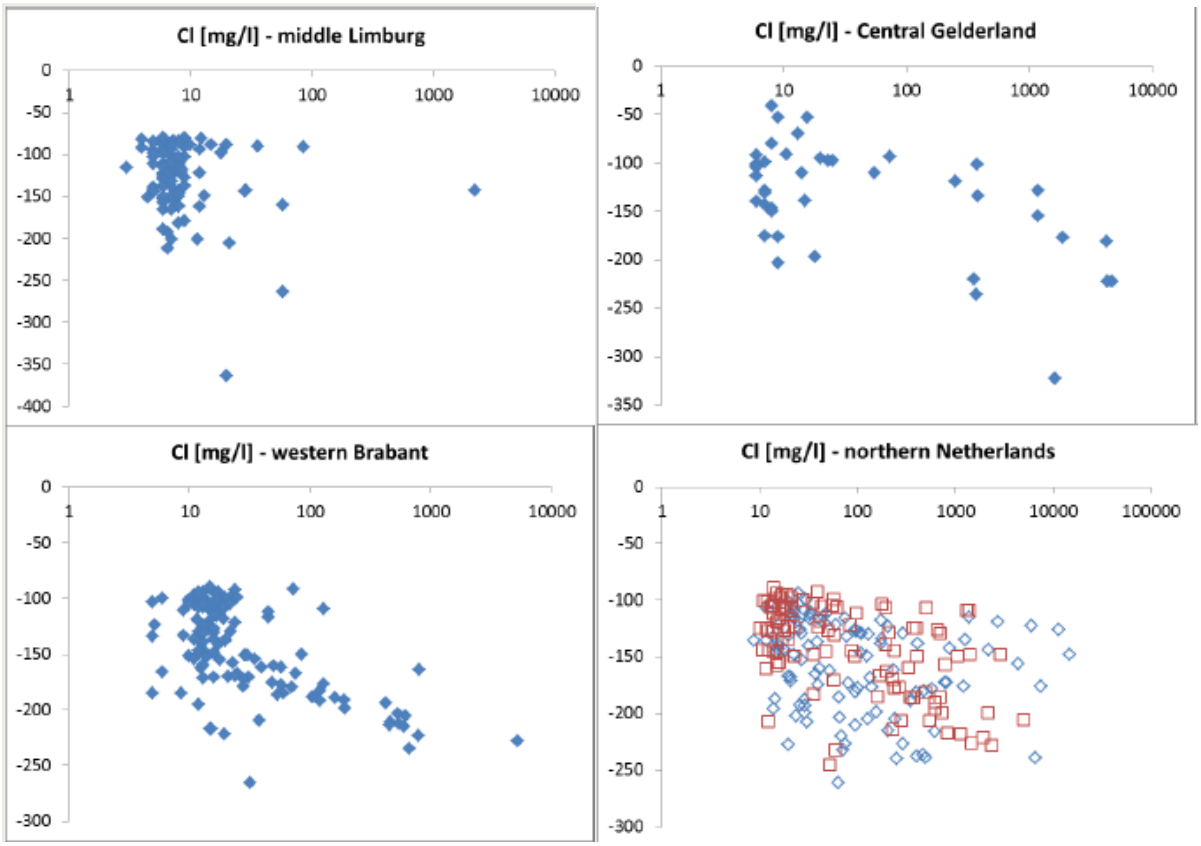

J. Grifjioen (2015). Concentration of Chloride in different locations of the Netherlands

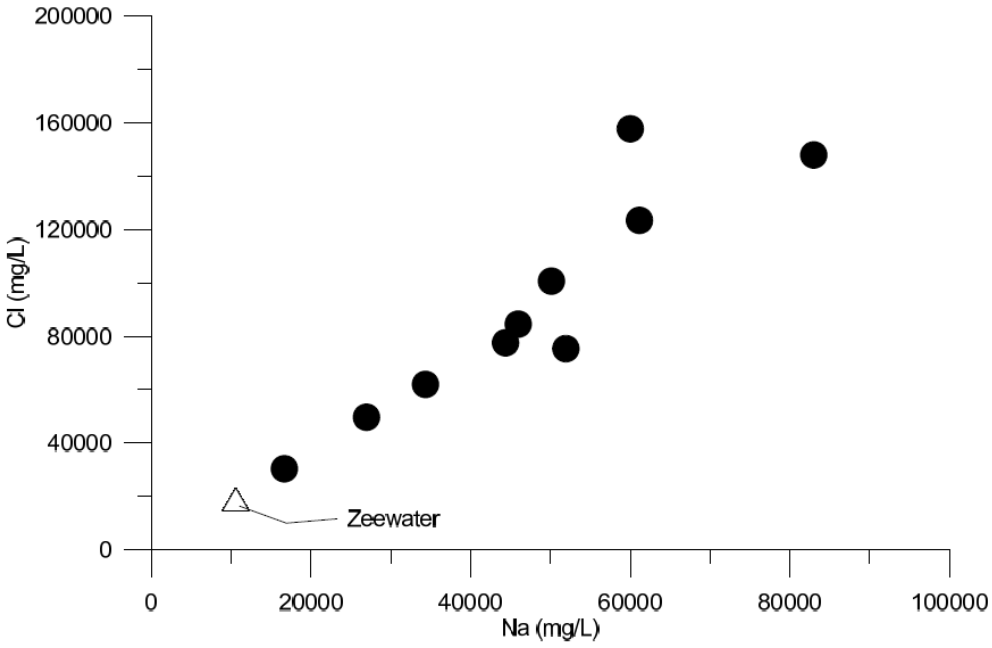

N. Hartog,(2016) Chloride and Nitrate concentration deep geothermal wells in the Netherlands from 1500 to 3000 m

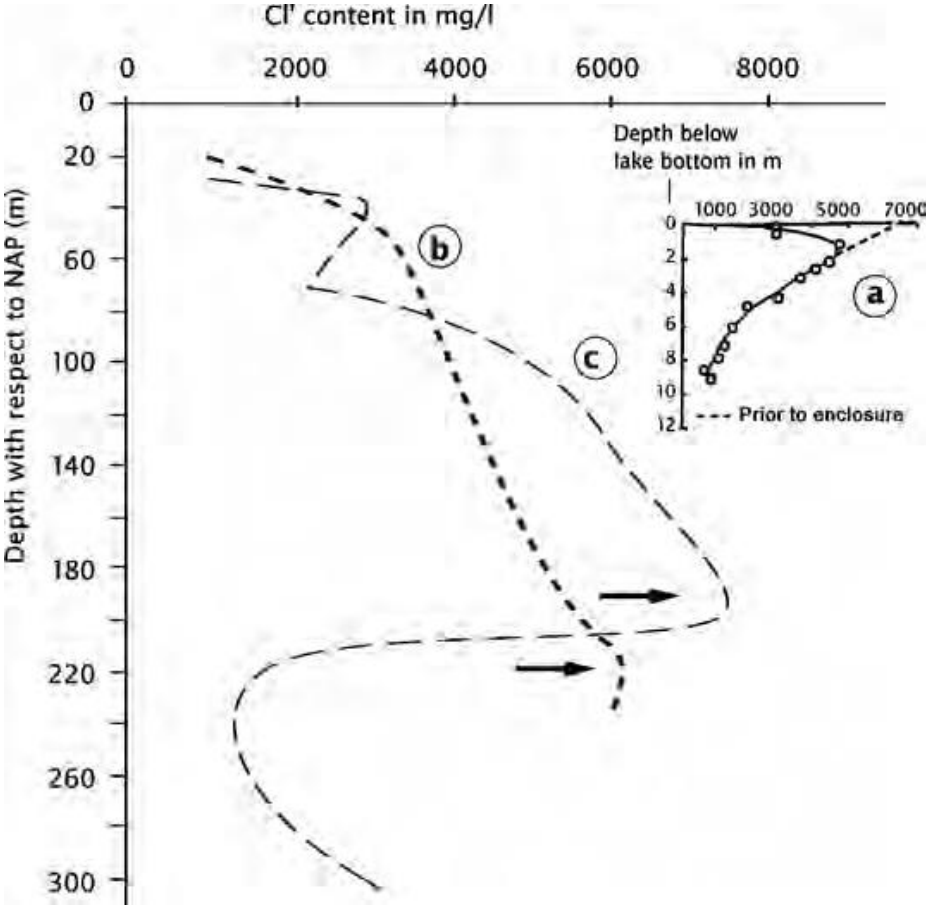

JJ. de Vries, Chloride concentration under the Haarlemmerpolder

Appendix [5] Salt gradient linearization based on deep geothermal wells salt concentrations

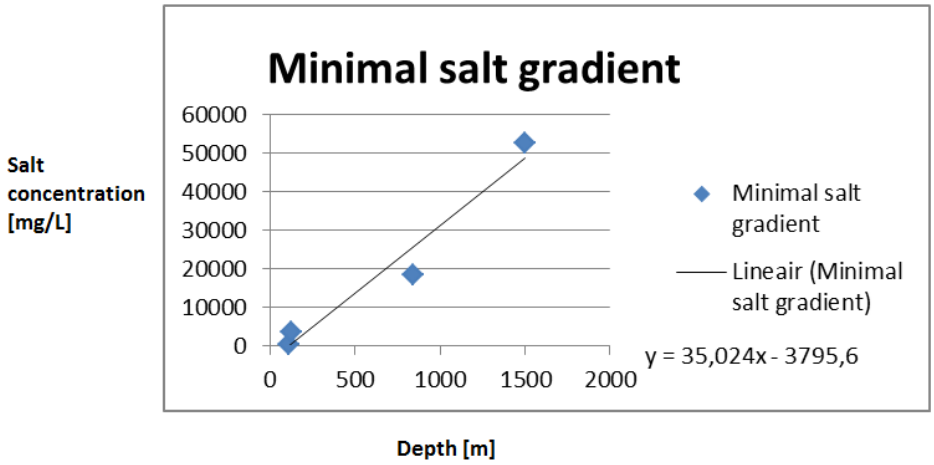

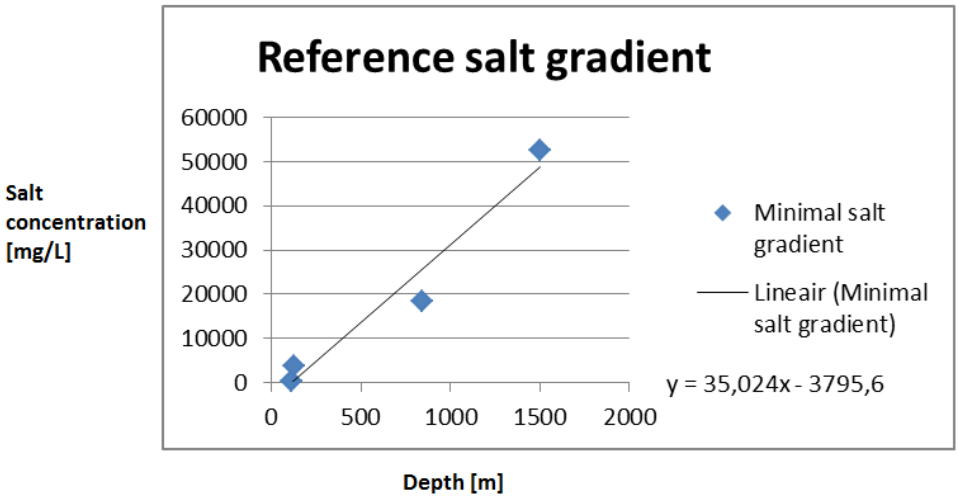

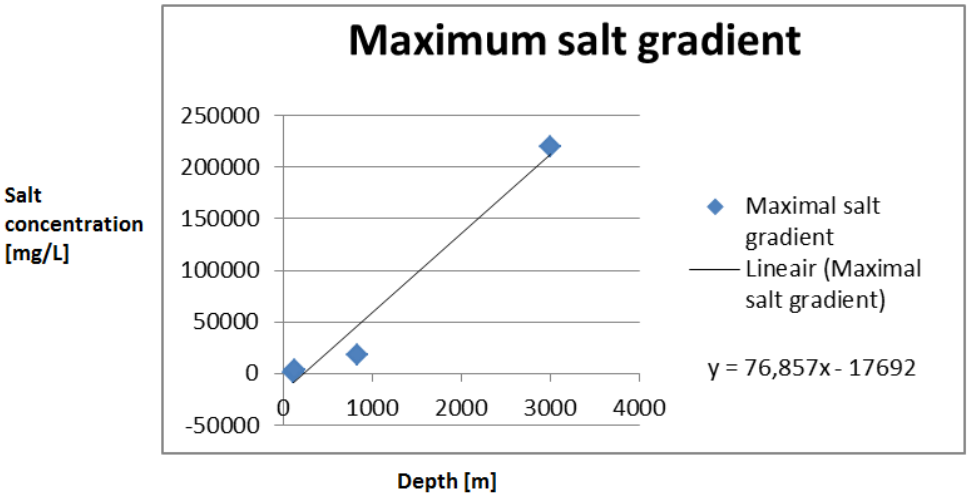

Appendix [6] Tilting time parameters and predicitons for different values of hydraulic conductivity and salinity gradient

	Unnamed layer	Berg Sand	Texel Member
Water density at storage [kg/m^3]	986,635383	989,762115	991,5130839
Water density in ambient layer [kg/m^3]	1002,5885	1004,97726	1006,182494
Storage temperature [C]	60	60	60
Salinity[-]	4,65	8,90	11,28
Average depth of aquifer [m]	170	420	560
Temperature in layer [C]	14,4	19,4	22,2
Salt concentration [kg/m^3]	4,65	8,90	11,28
Ambient viscosity [kg/m day]	1,3466E-08	1,1967E-08	1,12508E-08
Viscosity during storage [kg/m s]	5,4552E-09	5,5498E-09	5,60279E-09
H [m]	20	20	20
Kh [m2]	8,31E-12	8,31E-12	8,31E-12
Kv [m2]	8,31E-16	8,31E-16	8,31E-16
Ca[J/(m3*K)]	1,36E+06	1,36E+06	1,36E+06
Cw [J/(m3K)]	4,19E+03	4,20E+03	4,21E+03
to final (s)	3175953,68	3960478,11	4593877,504
to final (d)	37	46	53
Δto (d)	0	9	16
Time increase [%]	0	25	45

Table 4 Tilting time prediction for under boundary of hydraulic conductivity and salinity gradient of 17 mg/L

	Unnamed layer	Berg Sand	Texel Member
Water density at storage [kg/m^3]	986,635383	989,762115	991,5130839
Water density in ambient layer [kg/m^3]	1002,5885	1004,97726	1006,182494
Storage temperature [C]	60	60	60
Salinity[-]	4,65	8,90	11,28
Average depth of aquifer [m]	170	420	560
Temperature in layer [C]	14,4	19,4	22,2
Salt concentration [kg/m^3]	4,65	8,90	11,28
Ambient viscosity [kg/m day]	1,3466E-08	1,1967E-08	1,12508E-08
Viscosity during storage [kg/m s]	5,4552E-09	5,5498E-09	5,60279E-09
H [m]	20	20	20
Kh [m2]	4,155E-11	4,155E-11	4,155E-11
Kv [m2]	4,155E-14	4,155E-14	4,155E-14
Ca[J/(m3*K)]	1,36E+06	1,36E+06	1,36E+06
Cw [J/(m3K)]	4,19E+03	4,20E+03	4,21E+03
to final (s)	200864,948	250482,629	290542,3241
to final (d)	2	3	3
Δto (d)	0	1	1
Time increase [%]	0	25	45

Table 5 Tilting time prediction for average hydraulic conductivity and salinity gradient of 17 mg/L

	Unnamed layer	Berg Sand	Texel Member
Water density at storage [kg/m^3]	986,635383	989,762115	991,5130839
Water density in ambient layer [kg/m^3]	1002,5885	1004,97726	1006,182494
Storage temperature [C]	60	60	60
Salinity[-]	4,65	8,90	11,28
Average depth of aquifer [m]	170	420	560
Temperature in layer [C]	14,4	19,4	22,2
Salt concentration [kg/m^3]	4,65	8,90	11,28
Ambient viscosity [kg/m day]	1,3466E-08	1,1967E-08	1,12508E-08
Viscosity during storage [kg/m s]	5,4552E-09	5,5498E-09	5,60279E-09
H [m]	20	20	20
Kh [m2]	8,31E-11	8,31E-11	8,31E-11
Kv [m2]	8,31E-13	8,31E-13	8,31E-13
Ca[J/(m3*K)]	1,36E+06	1,36E+06	1,36E+06
Cw [J/(m3K)]	4,19E+03	4,20E+03	4,21E+03
to final (s)	31759,5368	39604,7811	45938,77504
to final (d)	0	0	1
Δto (d)	0	0	0
Time increase [%]	0	25	45

Table 6 Tilting time prediction for upper boundary of hydraulic conductivity and salinity gradient of 17 mg/L

	Unnamed layer	Berg Sand	Texel Member
Water density at storage [kg/m^3]	987,297515	993,734901	997,3398329
Water density in ambient layer [kg/m^3]	1003,28741	1009,13131	1012,245315
Storage temperature [C]	60	60	60
Salinity[-]	5,55	14,30	19,20
Average depth of aquifer [m]	170	420	560
Temperature in layer [C]	14,4	19,4	22,2
Salt concentration [kg/m^3]	5,55	14,30	19,20
Ambient viscosity [kg/m day]	1,3486E-08	1,2087E-08	1,14271E-08
Viscosity during storage [kg/m s]	5,4753E-09	5,67E-09	5,77907E-09
H [m]	20	20	20
Kh [m2]	8,31E-12	8,31E-12	8,31E-12
Kv [m2]	8,31E-16	8,31E-16	8,31E-16
Ca[J/(m3*K)]	1,36E+06	1,36E+06	1,36E+06
Cw [J/(m3K)]	4,20E+03	4,22E+03	4,23E+03
to final (s)	3173144,68	5334986,99	8590887,458
to final (d)	37	62	99
Δto (d)	0	25	63
Time increase [%]	0	68	171

Table 7 Tilting time prediction for lower boundary of hydraulic conductivity and salinity gradient of 35 mg/L

	Unnamed layer	Berg Sand	Texel Member
Water density at storage [kg/m^3]	987,297515	993,734901	997,3398329
Water density in ambient layer [kg/m^3]	1003,28741	1009,13131	1012,245315
Storage temperature [C]	60	60	60
Salinity[-]	5,55	14,30	19,20
Average depth of aquifer [m]	170	420	560
Temperature in layer [C]	14,4	19,4	22,2
Salt concentration [kg/m^3]	5,55	14,30	19,20
Ambient viscosity [kg/m day]	1,3486E-08	1,2087E-08	1,14271E-08
Viscosity during storage [kg/m s]	5,4753E-09	5,67E-09	5,77907E-09
H [m]	20	20	20
Kh [m2]	4,155E-11	4,155E-11	4,16E-11
Kv [m2]	4,155E-14	4,155E-14	4,16E-14
Ca[J/(m3*K)]	1,36E+06	1,36E+06	1,36E+06
Cw [J/(m3K)]	4,20E+03	4,22E+03	4,23E+03
to final (s)	200687,291	337414,204	543335,4298
to final (d)	2	4	6
Δto (d)	0	2	4
Time increase [%]	0	68	171

Table 8 Tilting time prediction for reference case of hydraulic conductivity and salinity gradient of 35 mg/L

	Unnamed layer	Berg Sand	Texel Member
Water density at storage [kg/m^3]	988,842488	1003,00472	1010,935552
Water density in ambient layer [kg/m^3]	1004,91821	1018,82409	1026,391893
Storage temperature [C]	60	60	60
Salinity[-]	7,65	26,90	37,68
Average depth of aquifer [m]	170	420	560
Temperature in layer [C]	14,4	19,4	22,2
Salt concentration [kg/m^3]	7,65	26,90	37,68
Ambient viscosity [kg/m day]	1,3533E-08	1,2367E-08	1,18384E-08
Viscosity during storage [kg/m s]	5,522E-09	5,9504E-09	6,19038E-09
H [m]	20	20	20
Kh [m2]	8,31E-12	8,31E-12	8,31E-12
Kv [m2]	8,31E-16	8,31E-16	8,31E-16
Ca[J/(m3*K)]	1,36E+06	1,36E+06	1,36E+06
Cw [J/(m3K)]	4,20E+03	4,26E+03	4,29E+03
to final (s)	3166616,08	26830415,1	-8573362,881
to final (d)	37	311	-99
Δto (d)	0	274	-136
Time increase [%]	0	747	-371

Table 9 Tilting time prediction for upper boundary of hydraulic conductivity and salinity gradient of 35 mg/L

	Unnamed layer	Berg Sand	Texel Member
Water density at storage [kg/m^3]	988,842488	1003,00472	1010,935552
Water density in ambient layer [kg/m^3]	1004,91821	1018,82409	1026,391893
Storage temperature [C]	60	60	60
Salinity[-]	7,65	26,90	37,68
Average depth of aquifer [m]	170	420	560
Temperature in layer [C]	14,4	19,4	22,2
Salt concentration [kg/m^3]	7,65	26,90	37,68
Ambient viscosity [kg/m day]	1,3533E-08	1,2367E-08	1,18384E-08
Viscosity during storage [kg/m s]	5,522E-09	5,9504E-09	6,19038E-09
H [m]	20	20	20
Kh [m2]	8,31E-12	8,31E-12	8,31E-12
Kv [m2]	8,31E-16	8,31E-16	8,31E-16
Ca[J/(m3*K)]	1,36E+06	1,36E+06	1,36E+06
Cw [J/(m3K)]	4,20E+03	4,26E+03	4,29E+03
to final (s)	3166616,08	26830415,1	-8573362,881
to final (d)	37	311	-99
Δto (d)	0	274	-136
Time increase [%]	0	747	-371

Table 10 Tilting time prediction for lower boundary of hydraulic conductivity and salinity gradient of 77 mg/L

	Unnamed layer	Berg Sand	Texel Member
Water density at storage [kg/m^3]	988,842488	1003,00472	1010,935552
Water density in ambient layer [kg/m^3]	1004,91821	1018,82409	1026,391893
Storage temperature [C]	60	60	60
Salinity[-]	7,65	26,90	37,68
Average depth of aquifer [m]	170	420	560
Temperature in layer [C]	14,4	19,4	22,2
Salt concentration [kg/m^3]	7,65	26,90	37,68
Ambient viscosity [kg/m day]	1,3533E-08	1,2367E-08	1,18384E-08
Viscosity during storage [kg/m s]	5,522E-09	5,9504E-09	6,19038E-09
H [m]	20	20	20
Kh [m2]	4,155E-11	4,155E-11	4,155E-11
Kv [m2]	4,155E-14	4,155E-14	4,155E-14
Ca[J/(m3*K)]	1,36E+06	1,36E+06	1,36E+06
Cw [J/(m3K)]	4,20E+03	4,26E+03	4,29E+03
to final (s)	200274,386	1696904,45	-542227,0782
to final (d)	2	20	-6
Δto (d)	0	17	-9
Time increase [%]	0	747	-371

Table 11 Tilting time prediction for reference case of hydraulic conductivity and salinity gradient of 77 mg/L

	Unnamed layer	Berg Sand	Texel Member
Water density at storage [kg/m^3]	988,842488	1003,00472	1010,935552
Water density in ambient layer [kg/m^3]	1004,91821	1018,82409	1026,391893
Storage temperature [C]	60	60	60
Salinity[-]	7,65	26,90	37,68
Average depth of aquifer [m]	170	420	560
Temperature in layer [C]	14,4	19,4	22,2
Salt concentration [kg/m^3]	7,65	26,90	37,68
Ambient viscosity [kg/m day]	1,3533E-08	1,2367E-08	1,18384E-08
Viscosity during storage [kg/m s]	5,522E-09	5,9504E-09	6,19038E-09
H [m]	20	20	20
Kh [m2]	8,31E-11	8,31E-11	8,31E-11
Kv [m2]	8,31E-13	8,31E-13	8,31E-13
Ca[J/(m3*K)]	1,36E+06	1,36E+06	1,36E+06
Cw [J/(m3K)]	4,20E+03	4,26E+03	4,29E+03
to final (s)	31666,1608	268304,151	-85733,62881
to final (d)	0	3	-1
Δto (d)	0	3	-1
Time increase [%]	0	747	-371

Tabel 12 Tilting time prediction for upper boundary of hydraulic conductivity and salinity gradient of 77 mg/L

Appendix [7] Titling time increase around the optimal density-compensation depth of 790m in the reference case

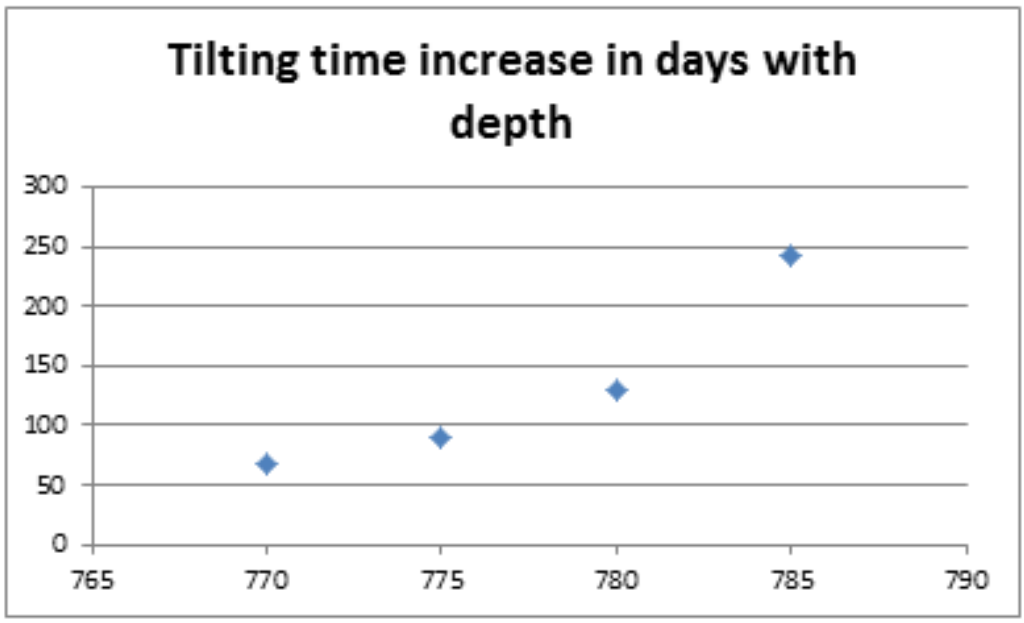

Bibliography

[i] Rijksoverheid (2017), Rijksoverheid stimuleert duurzame energie.19-06-2017 https://www.rijksoverheid.nl/onderwerpen/duurzame-energie/inhoud/meer-duurzame-energie-in-de-toekomst

[ii] Jong, K.d., 2016. Warmte in Nederland (heat in the Netherlands), Steenwijk.

[iii] Hartog N, Bloemendal M, Slingerland E, Van Wijk A (2016) Visie op warmtevoorziening

[iv] Delft Energy Initiative. Het delft plan, 14-02-2017. http://www.tudelft.nl/onderzoek/thematische-samenwerking/delft-research-based-initiatives/delft-energy-initiative/het-delft-plan/.

[v] Delft Aardwarmte Project. (2017). Delft Aardwarmte Project. [online] Available at: http://www.delftaardwarmteproject.nl/

[vi] Willemsen, N., 2016. Rapportage bodemenergiesystemen in Nederland. RVO / IF technology, Arnhem.

[vii] Dekker, L.d., (2016). Bepalende factoren voor goed functionerende WKO, kennisplatform bodemenergie.

[viii] Hacking, T., (2017). The Suitability of a High Temperature Aquifer Thermal Energy Storage on the TU-Delft Campus. TU-Delft

[ix] Sommer, W. (2007). Het effect van ruimtelijke dimensionering op het rendement van warmte-koude opslagsystemen. Almere: Witteveen + Bos.

[x] Calje, R. (2010) Future use of Aquifer Thermal Energy Storage below the historic centre of Amsterdam TU-Delft

[xi] Bloemendal, Hartog, van Wijk, 2016. Visie op Triplet

[xii] Energievastgoed. (2017). Dossier: Warmte en Koudeopslag (WKO) - Energievastgoed. 19-06-2017 http://www.energievastgoed.nl/dossiers/dossier-warmte-en-koude/

[xiii] Sommer, W. (2007). Het effect van ruimtelijke dimensionering op het rendement van warmte-koude

[xiv] Schout et al, (2014). Analysis of recovery efficiency in high-temperature aquifer thermal energy storage: a Rayleigh-based method,

[xv] Zeghici, R. M., Essink, G. H. O., Hartog, N., & Sommer, W. (2015). Integrated assessment of variable density–viscosity groundwater flow for a high temperature mono-well aquifer thermal energy storage (HT-ATES) system in a geothermal reservoir. Geothermics, 55, 58-68.

[xvi] Drijver, B. (2014). Thermisch rendement hoge & middelhoge temperatuur warmteopslag in de bodem. Belangrijkste leermomenten voor toekomstige tuinbouwprojecten. IF technology.

[xvii] Hartog, N. (2011). Literatuurstudie Meer Met Bodemenergie, Overzicht van kennis en onderzoeksvragen rondom warmte- en koudeopslag - Hoofdstuk 6: Effecten op geochemie. Bioclear, IF Technology, Deltares en Wageningen Universiteit, 2012.

[xviii] Brokx, L (2016). Problems encountered with and future possibilities for medium and high temperature aquifer thermal energy storage in the Netherlands. Utrecht Unitversity

[xix] Schout., Drijver, Schotting (2016). The influence of the injection temperature on the recovery efficiency of high temperature aquifer thermal energy storage: Comment on Jeon et al., 2015. Utrecht University, IF Technology

[xx] Kimbler, O.K., Kazmann, R.G., Whitehead, W.R., 1975. Cyclic Storage of Fresh Water in Saline Aquifers. Louisana State University, Baton Rouge, LA.

[xxi] Ward, Simmons, Dillon (2007). A theoretical analysis of mixed convection in aquifer storage and recovery: How important are density effects? Journal of Hydrology (2007) 343, 169– 186

[xxii] Lopik, Hartog, Zaadnoordijk (2016). The use of salinity contrast for density difference compensation to improve the thermal recovery efficiency in high-temperature aquifer thermal energy storage systems Hydrogeol J

[xxiii] Gutierrez-Neri M, Buik N, Drijver B, Godschalk B (2011) Analysis of recovery efficiency in a high-temperature energy storage system. Proceedings of the First National Congress on Geothermal Energy, Utrecht, The Netherlands, October 2011

[xxiv] Nield DA, Bejan A (1999) Convection in porous media, 2nd edn. Springer, New York

[xxv] Hellstrom, G., Tsang, C., Claesson, J. (1979). Heat storage in aquifers, Buoyancy flow and stratification problems. Lawrence Berkeley laboratory, University of California. 1979

[xxvi] Voss CI (1984) A finite-element simulation model for saturated-unsaturated, fluid-density-dependent ground-water flow with energy transport or chemically-reactive single-species solute transport. US Geol Surv Water Resour Invest Rep 84-4369

[xxvii] Mostafa H. Sharqawy , John H. Lienhard V & Syed M. Zubair (2010) Thermophysical properties of seawater: a review of existing correlations and data, Desalination and Water Treatment, 16:1-3, 354-380, DOI: 10.5004/dwt.2010.1079

[xxviii] Edelman, D. (2004) Temperaturen in de Nederlandse ondergrond.

[xxix] Griffioen, J.(2015) The composition of deep groundwater in the Netherlands in relation to disposal of radioactive waste, Opera TNO p 21-23

[xxx] De Vries, JJ. (2007) , Geology of the Netherland Royal Netherlands Academy of Arts and Sciences,p: 295–315

[xxxi] Hartog, N (2016), Risicos van Geothermie voor grondwater, BTO, Nieuwegein

[xxxii] K. N. Duggal, J. P. Son (1996)i: Elements of Water Resources Engineering. Publisher New Age International, p.270